Organic Geochemistry 43 (2012) 125–149

Contents lists available at SciVerse ScienceDirect

Organic Geochemistry

journal homepage: www.elsevier.com/locate/orggeochem

Palaeoclimate reconstruction from biomarker geochemistry and stable isotopes of *n*-alkanes from Carboniferous and Early Permian humic coals and limnic sediments in western and eastern Europe

A. Izart [a,*], F. Palhol [b], G. Gleixner [c], M. Elie [d], T. Blaise [a], I. Suarez-Ruiz [e], R.F. Sachsenhofer [f], V.A. Privalov [g], E.A. Panova [h]

[a] *UMR 7566 G2R, Université Henri Poincaré, BP23, F-54501 Vandoeuvre-les-Nancy, France*
[b] *CRPG-CNRS, 15 rue Notre-Dame-des-Pauvres, BP 20, F-54501 Vandoeuvre-les-Nancy, France*
[c] *Max-Planck-Institut für Biogeochemie, Jena, Germany*
[d] *Sarawak Shell Berhad, Locked Bag No. 1, 98009 Lutong, Sarawak, Malaysia*
[e] *Instituto Nacional del Carbon, INCAR, CSIC Ap. Co. 73, 33080 Oviedo, Spain*
[f] *University of Leoben, Peter Tunner Strasse 5, A-8700 Leoben, Austria*
[g] *Donetsk National Technical University, Artem Street 58, UA-83000 Donetsk, Ukraine*
[h] *UkrNIMI, National Academy of Sciences of Ukraine, Tchelyskintsev Street 291, UA-83121 Donetsk, Ukraine*

ARTICLE INFO

Article history:
Received 16 May 2011
Received in revised form 4 October 2011
Accepted 6 October 2011
Available online 14 October 2011

ABSTRACT

The type of organic matter (OM) in European Carboniferous and Permian swamp and lake sediments from the Carboniferous and Permian was determined using organic petrography, Rock–Eval data and biomarker distributions. Coals deposited in swamps contain humic OM formed under oxic conditions. Boghead coals and black shales deposited in lakes contain a mixture of algal and humic OM formed under reducing conditions. Diterpanes and previous palaeobotanic studies constrain the species of plants living near the lacustrine shore or in the swamp during deposition, allowing the palaeoclimate to be inferred. During the Carboniferous, the climate was not always tropical wet, as some periods of dryness are evident from the sedimentology, palaeobotany and organic geochemistry. During the Permian, the climate was not always tropical dry as some periods of wetness associated with the monsoons are recorded (Roscher, M., Schneider, J.W., 2006. Permocarboniferous climate: Early Pennsylvanian to Late Permian climate development of central Europe in a regional and global context. In: Lucas, S.G., Cassini, G., Schneider, J.W. (Eds.), Non-Marine Permian Chronology and Correlation, vol. 265. The Geological Society of London, pp. 95–136). The appearance of xerophyte plants from the Stephanian was also recorded by way of aromatic hydrocarbons, retene for gymnosperms and arborane/fernane for cordaites and probably seed ferns. Cycles of wetness and dryness for Europe during the Carboniferous and Permian are proposed on the basis of comparison of aliphatic and aromatic hydrocarbons.

δD values provided information on the palaeotemperature of the air in the swamps and water in lakes, as well as palaeoclimate. Values of ca. −100‰ seen in the Carboniferous coals and Permian limnic deposits are indicative of a tropical climate, in contrast to a glacial or temperate climate, where the values are ca. −200‰. The value for Carboniferous coals could result from high evapotranspiration of plants living under a wet tropical climate vs. a temperate climate. During the Early Permian the climate was dry tropical. For such samples, the δD values for the *n*-alkanes derived from lacustrine algae were depleted in D relative to the values for the *n*-alkanes derived from terrestrial higher plants, attributed to the higher evapotranspiration on land than evaporation from the lake. Alternatively, the xerophytic plants that drifted into the lake via a river could have grown during a dry phase and the autochthonous algae bloomed during a wet phase.

1. Introduction

This study investigates the interaction between climate and organic matter (OM) in western and eastern Europe during the Early Carboniferous to Early Permian when the climate cycled through a wet/dry tropical state. Shifts in climate occurred as the European plate drifted towards the north, as exhibited by maps of the Moscovian (Late Carboniferous, Fig. 1: Dercourt et al., 2000) and Artinskian (Early Permian, Fig. 2: Dercourt et al., 2000). The goal of this study was to determine whether palaeoclimatic and palaeobotanic changes were revealed in biomarker geochemistry and their compound specific stable isotopes.

* Corresponding author. Tel.: +33 3 87 66 20 12; fax: +33 3 87 37 86 07.
E-mail address: izart.alain@voila.fr (A. Izart).

0146-6380/$ - see front matter © 2011 Elsevier Ltd. All rights reserved.
doi:10.1016/j.orggeochem.2011.10.004

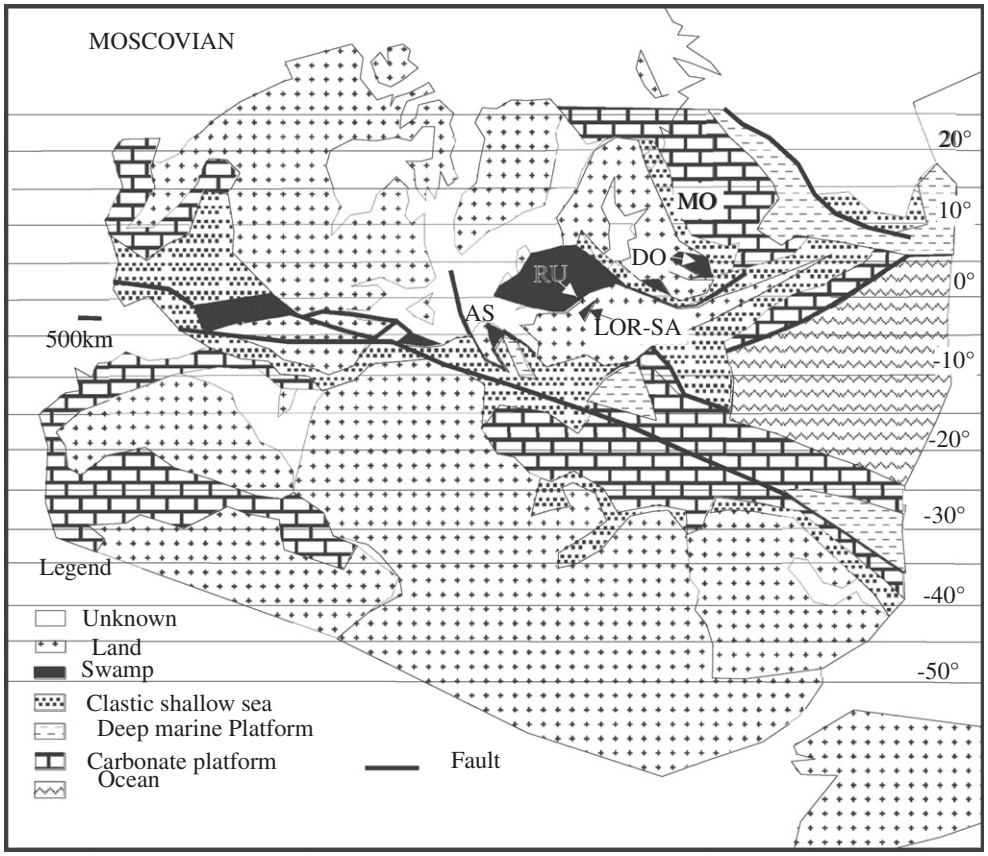

Fig. 1. Location of basins on the Moscovian map (modified after Dercourt et al. (2000)). AS, Asturias; DO, Donets; LOR-SA, Lorraine-Saar; MO, Moscow; RU, Ruhr.

The basins of western and eastern Europe were located at 10°S during the Viséan, between the Equator and 5°N during the Moscovian, and between 5°N and 10°N during the Early Permian (Golonka et al., 1995; Dercourt et al., 2000). During the Moscovian, the Euramerican flora (Izart et al., 1998; Vai, 2003) in the basins was related to the equatorial and a tropical ever-wet biome (Ziegler, 1990), with a rainforest of hygrophytic plants fitting well with the palaeoequatorial belt in the Moscovian map. During the Early Permian, the Euramerican flora was related to the tropical and subtropical summer wet biome, with alternation of hygrophytic and xerophytic plants, and limnic black shales explained by a dryer climate with a monsoon period (Roscher and Schneider, 2006). Palaeobotany shows the presence of land plants consistent with a wet tropical climate (arborescent ferns, pteridosperms and lycopods) during the Late Carboniferous and the progressive appearance of dry tropical plants (conifers) during the Late Carboniferous (Kasimovian, Gzhelian, Stephanian and Autunian) and their predominance during the Early Permian (Asselian, Late Autunian).

On different timescales, from years to million of years, proof of climatic change has been observed in the Carboniferous and Permian sediments. Laminated black shale of perennial lakes deposited during the Permian in the Saar Basin has been interpreted as the result of annual changes in wet and dry seasons of a monsoonal climate (Schneider et al., 2006). Müller et al. (2006) showed that changes in $\delta^{13}C$ and $\delta^{18}O$ values for dolomites deposited in Permian lakes from the Saar Basin reflect an increase in water input or an increase in evaporation. Lake level increased from low at the base to high at the middle, then decreased to a low level at the top of the black shale. Twenty black shales are known in the Glan group of the Saar Basin corresponding to a cyclicity of ca. 400 ka.

Cecil et al. (2003) modelled the global palaeoclimate during the Middle Pennsylvanian (306 Ma). Within a glacial interval with continental ice in the southern hemisphere, climatic conditions limited the southern excursion of the intertropical convergence zone (ITCZ) during the southern hemisphere summer (northern hemisphere winter) and created a relatively narrow equatorial low pressure rainy belt (doldrums). For this reason, coals and the weathering of palaeosol associated with a wet period can be observed during lowstands in the northern American basins. Within an interglacial interval, the annual cross-equatorial movement of the ITCZ towards the north during the north hemisphere summer and towards the south during the south hemisphere summer resulted in a significant increase in both dryness and seasonality of the rainfall in low latitudes. For this reason, marine limestones associated with a dry period can be observed during transgression and highstands in the northern American basins.

An ever-wet tropical zone was not developed at low latitude from Stephanian to the Permian. The seasonality within the tropics was reported by Ziegler (1990) and modelled by Parrish (1993, 1995) and Kutzbach and Ziegler (1993, 1994). The wide shift in the ITCZ caused equatorial drought in summer and winter. During spring and autumn, a wet period occurred, while the ITCZ was centred over the equator. The occurrence of coals decreased during this period. Laminated black shale of perennial lake origin was interpreted as a result of annual changes in the wet and dry seasons of the monsoonal climate (Schneider et al., 2006). Müller et al. (2006) showed that the level of the Permian lake changed and was at a maximum in the middle part of black shale. Dry and wet phases described by Roscher and Schneider (2006), and confirmed by our study, fit well with, respectively, glaciation and deglaciation phases on Gondwana (Lopez-Gamundi, 1997; Visser, 1997; Bangert et al., 1999; Iannuzi and Rösler, 2000; Stollhofen et al., 2000). The biomarker distributions for high frequency sequences from the Donets Basin (Izart et al., 2006) support the

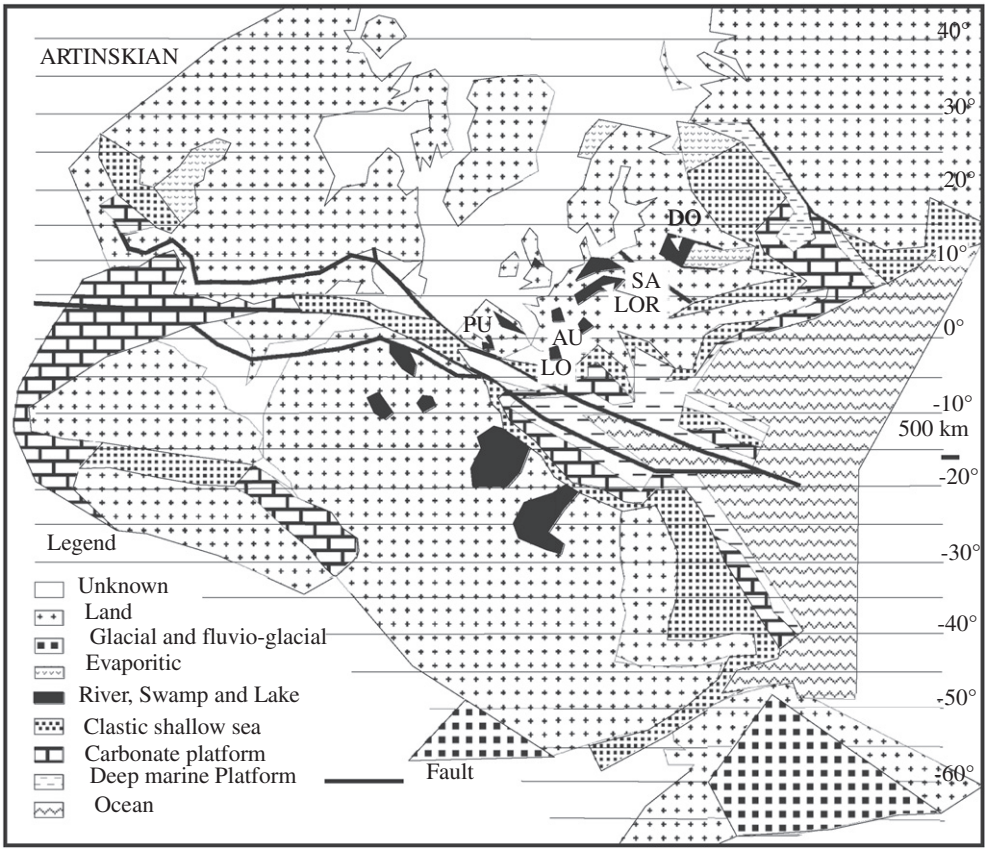

Fig. 2. Location of basins in the Artinskian map (modified after Dercourt et al. (2000)). AU, Autun and Buxieres; DO, Donets; LO, Lodève; LOR, Lorraine; PU, Puertollano; SA, Saar.

palaeoclimatic model of Cecil et al. (2003): an intermediate climate during a lowstand system tract (LST, sandstone), a wet climate during early transgressive system tract (palaeosol and coal), a dry climate during late transgressive system tract (TST, limestone), maximum flooding surface (MFS, claystone) and highstand system tract (HST, deltaic siltstone). The biomarker distributions for second order sequences (10 Ma), third order sequences (1 Ma) and fourth order sequences (400 ka) during coal deposition in the Donets Basin showed a dry palaeoclimate during LST, intermediate or wet during TST and MFS, and wet during HST.

The alternation of wet and dry seasons in the tropical zone was modelled by Kutzbach and Ziegler (1993, 1994) and Parrish (1993, 1995) and explained by way of the wide shift in the ITCZ. Gibbs et al. (2002) modelled the Permian climate during the Sakmarian (280 Ma) and Wordian (260 Ma) and found distinctive seasonality and high aridity on the continents. Using sedimentological and palaeontological arguments, Schneider et al. (2006) and Roscher and Schneider (2006) determined successive periods of dryness and wetness during the Permian. Roscher et al. (2008) also modelled a tropical seasonal climate for western Europe during the Permian. Peyser and Poulsen (2008) modelled the controls on Permo-Carboniferous precipitation over tropical Pangea. They showed that the precipitation rate (PR) in the equator and northern hemisphere (10°N) depended on the significant extension of ice on Gondwana. Significant extension of ice occurred with a high PR of 1000 to 1400 mm yr^{-1} during the Carboniferous. Low extension of ice occurred with low PR of 800–1000 mm yr^{-1} during the Early Permian. Either deglaciation or a CO_2 increase could have caused a dry climate in low latitudes. Berner (1998) modelled an effectively low level of CO_2 during the Carboniferous as a result of the storage of CO_2 in coal and an increase during the Permian resulting from the release of CO_2 to the atmosphere following heating of coal and gas migration in coal basins. The radiochronological data chart from Menning and Hendrich (2002) was used for the Carboniferous and Permian.

2. Samples and analytical methods

Table 1 lists the samples and their location, as well as the macerals, vitrinite reflectance, Rock–Eval data and biomarker ratios. The samples are either humic coals representative of swamp deposits, or boghead (algal) coals and black shales representative of lake deposits.

Two bogheads (4525 a and b) were studied from the Early Carboniferous (Viséan) from the Moscow Basin (Russia) deposited in a lake during a period of alternating dry and humid tropical climate (Scotese and McKerrow, 1990). Five bogheads (E48985–E48989) from the Moscow Basin with diverse proportions of vitrinite and algae were analyzed by Armstroff (2004) and Armstroff et al. (2006) and are listed in Table 1 for comparison. The Moscow Basin (Figs. 1 and 2) was a marine platform during the Carboniferous and Early Permian (Makhlina et al., 1993; Izart et al., 1998, 2003) with alternating continental deposits during low stands and carbonated marine deposits formed during a transgressive and sea level high stand. Volkova (1975) studied the Kimov coal seam (Fig. 3) that contains vitrinite, fusinite and liptinite (spores and algae) macerals. Our two samples from the Volkova (1975) study were located in this column.

Coals rich in vitrinite and other sediments from the Donets Basin (Ukraine; Figs. 4 and 5) from the Early Carboniferous (Serpukhovian) to the Late Carboniferous (Bashkirian, Moscovian, Kasimovian and

Table 1
Biomarker, Rock–Eval and petrography data.[a]

Sample	Locality	Age	Lithology	Climate	M	VR	T_{max}	HI	OI	Ali	Aro	Pol	A	B	C	D	Pr/Ph	Pr/C17	Ph/C18	CPI
LC1A	Lodeve	Autunian	LBS	HDT	LV		428	153	28	23	53	24					0.6	0.45	0.39	1
LC3A	Lodeve	Autunian	LBS	HDT	LV		460	54	58	13	43	44					0.76	0.37	0.45	
LC4	Lodeve	Autunian	LBS	HDT	LV		425	268	23	52	25	23					1.22	1.32	0.67	0.7
LC17A	Lodeve	Autunian	LBS	HDT	LV		439	68	134	16	69	15					0.63	0.09	0.07	1
LC23A	Lodeve	Autunian	LBS	HDT	LV		436	179	18	52	24	24					1.09	0.59	0.58	1.2
LC24A	Lodeve	Autunian	LBS	HDT	LV		438	247	22	47	24	29					1.57	0.6	0.6	1.2
LC28	Lodeve	Autunian	LBS	HDT	LV		432	105	89	45	27	28					1.09	0.68	0.48	
LC30A	Lodeve	Autunian	LBS	HDT	LV		440	287	19	46	19	35					0.89	0.57	0.61	1
MA1 112.5	Münster	Autunian	LBS	HDT	LV	0.6	423	108	42				28	28	25	19	1.38	1.15	1.47	1.4
MA1 114.0	Münster	Autunian	LBS	HDT	LV	0.6	431	121	18				30	29	25	16	1	0.23	0.23	1.2
MA1 114.23	Münster	Autunian	LBS	HDT	LV	0.6	431	122					16	28	39	17	1.2	0.3	0.22	1.2
MA1 114.38	Münster	Autunian	LBS	HDT	LV	0.6	433	167	11	45	12	43	28	26	29	17	1	0.25	0.3	1.2
MA1 114.74	Münster	Autunian	LBS	HDT	LV	0.6	434	349	13				19	24	35	22	0.2	0.05	0.23	1.1
MA1 114.95	Münster	Autunian	LBS	HDT	LV	0.6	435	487	13				18	27	36	19	1.24	0.19	0.14	1.1
MA1 116.33	Münster	Autunian	LBS	HDT	LV	0.6	431	242	39				25	32	26	17	1.31	0.51	0.5	1.2
MA1 118.66	Münster	Autunian	LBS	HDT	LV	0.6	436	55	15				22	20	24	34	1.97	0.82	0.48	1.4
GW1449.70	Gehrweiler	Autunian	LBS	HDT	LV	0.6	438	70	15	55	12	33	8	20	38	34	1.04	0.22	0.16	1.1
OH46.01	Odernheim	Autunian	LBS	HDT	LV	0.6	436	160	23				14	56	19	11	1.1	0.27	0.25	1.2
OH46.40	Odernheim	Autunian	LBS	HDT	LV	0.6	436	160	20				21	24	34	21	1.1	0.5	0.4	1.1
OH47.69	Odernheim	Autunian	LBS	HDT	LV	0.6	435	330	31				9	13	45	33	0.94	0.16	0.15	1.2
AU1	Autun	Autunian	BC	HDT	LV	0.55	452	779	16	33	10	57	30	22	25	23	1.36	0.53	0.37	0.9
BX3	Buxieres	Autunian	HC	HDT	V	0.43	430	334	34	8	35	57	9	11	27	53	10.37	7.2	1.08	1.4
BX7	Buxieres	Autunian	LBS	HDT	LV		435	464	14	25	28	47	13	17	36	34	2.43	3.3	1.35	1.3
P29960	Puertollano	Stephanian	HC	HT	VILS	0.64				8	18	74		45	29	26	9.1	9.69	1.27	1.4
P29950	Puertollano	Stephanian	HC	HT	VILS	0.67				7	19	74		41	27	32	8.72	6.6	0.71	1.5
P29945	Puertollano	Stephanian	HC	HT	VILS	0.69				12	15	73		37	33	30	5.83	2.13	0.42	1.4
PB	Puertollano	Stephanian	LBS	HT	L	0.43				40	25	35	7	13	28	52	2.22	1.43	0.57	1.2
p5 Lug	Donets	Gzhelian	HC	HDT	V		433	325		21	32	47	44	22	23	11	3.8	5.2	1.9	1.4
o2 Svet	Donets	Kasimovian	HC	HDT	V	0.48	441	55		2	1	97	8	16	29	47	4.9	7.9	1.9	1.2
n36MC	Donets	Kasimovian	HC	HDT	V	0.63	431	243		9	32	59	22	8	21	49	8.9		1.4	1.2
n23MC	Donets	Kasimovian	HC	HT	V	0.65	431	231		7	39	54	23	9	20	48	7.3		1.3	1.2
n22MC	Donets	Kasimovian	HC	HT	V	0.7	432	258		8	45	47	19	32	24	25			1	1.2
5n1But	Donets	Myachkovian	HC	HT	V	0.63	436	305		8	37	55	31	28	29	12	9.3	10.8	1.1	1.2
4n1But	Donets	Myachkovian	HC	HT	V	0.75	438	244		3	14	83	35	32	24	9	7.6	5.5	0.7	1.1
3n1But	Donets	Myachkovian	HC	HT	V	0.79	444	262		5	29	66	34	37	22	7	7.7	3.4	0.5	1.2
2n1But	Donets	Myachkovian	HC	HT	V	0.83	442	255		6	22	72	36	34	22	8	7.3	4.3	0.6	1.2
1n1But	Donets	Myachkovian	HC	HT	V	0.84	437	254		5	25	75	30	35	23	12	6.9	3.1	0.5	1.2
m3Trudo	Donets	Podolskian	HC	HT	V	0.39	418	219		14	31	55	45	15	24	16	5.5	7.3	1.6	1.5
m2Bel	Donets	Podolskian	HC	HT	V	0.71	433	290		6	34	60	48	22	20	10	9	13.3	1.6	1.2
l4 Trudo	Donets	Kashirian	HC	HT	V	0.52	431	165		10	32	58	53	14	18	15	10.6	14	1.6	1.4
9l1 Dim	Donets	Kashirian	HC	HT	V	0.71	442	245		6	28	66	28	32	27	13	6	5.4	0.9	1.1
8l1 Dim	Donets	Kashirian	HC	HT	V	0.72	443	224		6	14	80	16	20	26	38	6.2	5.8	1	1
6l1 Dim	Donets	Kashirian	HC	HT	V	0.74	442	242		5	25	70	39	21	25	15	6.6	4.5	0.7	1.2
5l1 Dim	Donets	Kashirian	HC	HT	V	0.73	442	248		6	26	68	33	31	24	12	7.6	5.8	0.8	1.2
4l1 Dim	Donets	Kashirian	HC	HT	V	0.76	441	250		6	31	63	36	33	20	11	7.2	4.3	0.7	1.1
3l1 Dim	Donets	Kashirian	HC	HT	V	0.77	439	263		9	30	61	17	30	35	18	5.8	5.6	0.8	1.1
2l1 Dim	Donets	Kashirian	HC	HT	V	0.76	440	253		6	27	67	11	32	40	17	5.2	6.1	0.8	1.2
1l1 Dim	Donets	Kashirian	HC	HT	V	0.74	438	248	4	7	25	68	29	36	25	10	6.6	6.1	1	1.1
1k8 Nov	Donets	Kashirian	HC	HT	V	0.62	429	282		5	19	76	10	32	39	19	4.2	7.6	1.3	1.2
2 k22 Ka	Donets	Vereian	HC	HDT	V	1.03	468	157		13	52	35	11	36	37	16	2 2	0.5	0.3	1.1
1 k22 Ka	Donets	Vereian	HC	HDT	V	1.04	464	95		9	58	34	58	19	16	7	2	0.7	0.3	1.1
3 h10 Pe	Donets	Bashkirian	HC	HDT	V	0.63	438	243		22	39	39	14	8	29	49	7.5		0.8	1.4
2 h10 Pe	Donets	Bashkirian	HC	HDT	V	0.62	441	304		12	36	52	31	10	24	35	7.9		0.7	1.2
c11 YD	Donets	Serpukhovian	HC	HDT	V	0.7	436	249		12	34	54	3	18	47	32	5.9	10.5	1	1.2
2 c10 YD	Donets	Serpukhovian	HC	HDT	V	0.62	430	260	5	4	24	72	18	9	33	40	21.9		0.3	1.3
1 c10 YD	Donets	Serpukhovian	HC	HDT	VLS	0.63	431	229		11	38	51	17	34	37	12	9.5	3.8	0.4	1.6
4525 a	Moscow	Visean	BC	HDT	LV	0.35	438	435	63	6		92	8	10	18	64	1.17	0.32	0.32	1.4
4525 b	Moscow	Visean	BC	HDT	LV	0.35	439	426	67	7	5	88	4	7	19	70	1.78	0.53	0.28	1.6
E48985	Moscow	Visean	BC	HDT	LV	0.42							1	4	31	64	0.5	0.74	1.25	1.6
E48986	Moscow	Visean	BC	HDT	LV	0.39							2	10	18	70	1	0.37	0.35	1.7
E48987	Moscow	Visean	BC	HDT	LV	0.32							1	7	36	56	0.8	0.16	0.15	1.8
E48988	Moscow	Visean	BC	HDT	LV	0.41							3	36	34	27	0.6	0.84	0.96	0.9
E48989	Moscow	Visean	BC	HDT	LV	0.37							1	1	3	95	0.8	0.45	0.53	

[a] A, C_{12-16} *n*-alkanes; Ali, aliphatics; Ar, aromatics; B, C_{17-19} *n*-alkanes; BC, boghead coal; C, C_{20-24} *n*-alkanes; D, C_{25-35} *n*-alkanes; DT, dry tropical climate; HC, humic coal; HDT, humid-dry tropical climate; HI, hydrogen index (mg HC/g TOC); HT, humid tropical climate; L, liptinite (algae); LBS, lacustrine black shale; LS, liptinite (spores); M, macerals; Ph/C18, phytane/*n*-C_{18}; Pol, polars; Pr/C17, pristane/*n*-C_{17}; Pr/Ph, pristane/phytane; T_{max}, Rock–Eval T_{max} (°C); V, vitrinite; VR, measured vitrinite reflectance (%).

Gzhelian) were studied by Sachsenhofer et al. (2003) and Izart et al. (2006). They were deposited in swamps during a period of a humid tropical climate. Of the 52 coals previously studied using molecular approaches, 29 samples of lower maturity are listed in Table 1. The Donets Basin (Figs. 1 and 2) was a paralic coal basin and a rift developed during the Carboniferous and Early Permian (Izart et al., 1998, 2003, 2006; Alsaab et al., 2008), resulting in a thick sequence (15 km) of alternating continental deposits (fluvial sandstone and coal) during low stands and marine deposits (limestone, claystone and deltaic siltstone) during transgressive and high stands.

Three coal samples (P 29960, 29950 and 29945) studied by us and one black shale (PB) studied by Kruge and Suarez-Ruiz

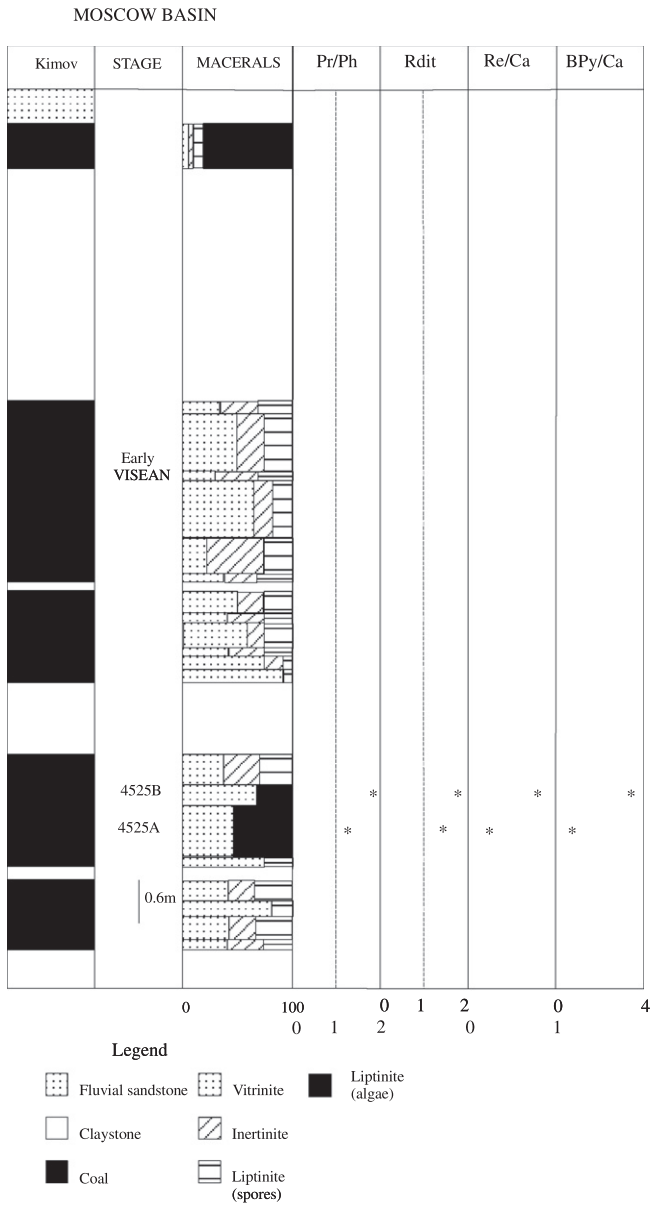

Fig. 3. Lithostratigraphic column of Viséan coals from Moscow Basin (modified after Volkova (1975)). BPy/Ca, benzopyrenes/cadalene; Pr/Ph, pristane/phytane; R_{dit}, diterpanes ratio; Re/Ca, retene/cadalene.

(1991), Del Rio et al. (1994) and Jimenez et al. (1999) are from the Late Stephanian in the Puertollano Basin (Spain; Fig. 6). Three samples, a coal (BX3), a boghead coal (AU1) and a black shale (BX7) are from the Late Carboniferous and Early Permian (Autunian) in France (Autun and Buxieres basins; Fig. 7). Twelve black shale samples are from the Early Permian (Autunian) in Germany (Saar Basin; Fig. 8). Six are from studies of *n*-alkanes conducted by Müller et al. (2006) and Müller (2007) and six from our studies of samples from the Münsterappel 1 (MA1), Gehrweiler 1 (GW1) and Odernheim–Hellersberg (OH) boreholes described by Müller et al. (2006). Samples of black shales from the Late Autunian of the Lodève Basin (Fig. 9) are from studies of *n*-alkanes, hopanes and steranes by Schlepp et al. (2001), who subdivided their samples in two groups named A and B. The Autun, Buxieres, Puertollano, Lorraine, Saar and Lodève basins (Figs. 1 and 2) are limnic intramontane basins, with deposits of coals, detritic rocks and lacustrine black shales during the Carboniferous and Permian (Izart et al., 1998, 2003, 2005; Jimenez et al., 1999; Schneider et al., 2006). Coals from the Westphalian and Stephanian in the Lorraine Basin were studied by Fleck (2001), Fleck et al. (2001) and Izart et al. (2005) and in the Saar Basin by Vliex et al. (1994). The OM was deposited in rare swamps and abundant lakes during a period of a dry tropical climate with alternating monsoons during the Late Stephanian and Early Permian.

Macerals and vitrinite reflectance at random orientation of particles (VRr) were studied in the Leoben laboratory using a Leitz microscope for the Donets coals (Sachsenhofer et al., 2003) and in the Oviedo laboratory using a MPV-Combi Leitz microscope for the bogheads and coals from the other basins. Rock–Eval pyrolysis was performed using a Rock–Eval 2+ instrument in the Leoben laboratory for the Donets coals and a Vinci Rock–Eval 6 instrument at the ISTO laboratory (Orléans, France) for the limnic samples. Rock–Eval data for the black shales from Saar came from Müller (2007). To characterize the molecular distributions, the powdered whole sediments were extracted with CH_2Cl_2 using a Dionex ASE instrument programmed at 100 °C. The extracts were fractionated using liquid chromatography on a silica column into saturated and aromatic hydrocarbon and polar fractions. Gas chromatography-mass spectrometry (GC–MS) analysis of the saturated and aromatic hydrocarbons fractions was performed at the UMR G2R laboratory (Nancy, France) using a Hewlett–Packard 5890 Series II gas chromatograph coupled to a HP 5971 mass-selective detector (MSD), operating in full scan (FULL) mode or single ion monitoring (SIM) mode. Peak areas from the SIM mass chromatograms were measured and the ratios of various biomarkers calculated (Tables 1 and 2). Representative chromatograms for saturated and aromatic fractions from coals, bogheads and black shales are shown in Fig. 13 and peak assignment for the hopanes and steranes are listed in Table 3. Others chromatograms for saturated hydrocarbons from coals from the Donets Basin and black shales from the Lodève Basin can be found in Sachsenhofer et al. (2003), Izart et al. (2006) and Schlepp et al. (2001).

An Isoprime isotopic ratio mass spectrometer coupled to a HP 6890 GC instrument was used to measure the stable hydrogen isotopic values of *n*-alkanes at the CRPG laboratory (Nancy, France). Four coal samples from the Late Carboniferous Donets Basin (2h10Pe, 1l1Dim, 1n5But and P5Lug) and one lacustrine sample from the Early Permian Autun Basin (AU1) were analyzed. Separation was achieved using a 30 m fused silica column (DB5-MS, 0.32 mm i.d., 0.25 μm film thickness). The oven temperature programme was: 50 °C (1 min) to 350 °C (held 29 min) at 5 °C/min. Ultra-high purity He was used as carrier gas at a constant flow of 0.5 ml/min. Samples were injected in the split mode with a split ratio of 1:1 and the injector temperature was 310 °C. Separated components were instantaneously converted to H_2 using a high temperature conversion system with chromium as catalyst at 1050 °C (Dawson et al., 2004) prior to analysis. All δD values are expressed in ‰ relative to the Vienna standard mean oceanic water (V-SMOW). In addition, three lacustrine samples from the Early Permian Saar Basin were measured at the Jena laboratory for δD values using an isotope ratio mass spectrometry (IRMS) instrument (Delta^{Plus} XL, Finnigan MAT, Bremen, Germany) coupled to a HP 5890 GC instrument.

The H_3^+ factor was determined in each run by observing the influence in the (m/z 3)/(m/z 2) signal ratio of H_2 for pulses at different pressure obtained by adjustment of the variable volume of the spectrometer. This factor was used to calculate a new (m/z 3) signal. The δD values were then obtained by integration of the ion beam signal collected on m/z 2 and corrected m/z 3 signal. A laboratory standard was used daily to calibrate the δD values of samples to the V-SMOW scale and to monitor the stability of the system (furnace and isotope ratio mass spectrometer).

Analytical uncertainty was estimated from replicate analyses. The laboratory standard was injected daily (6×) and the value used

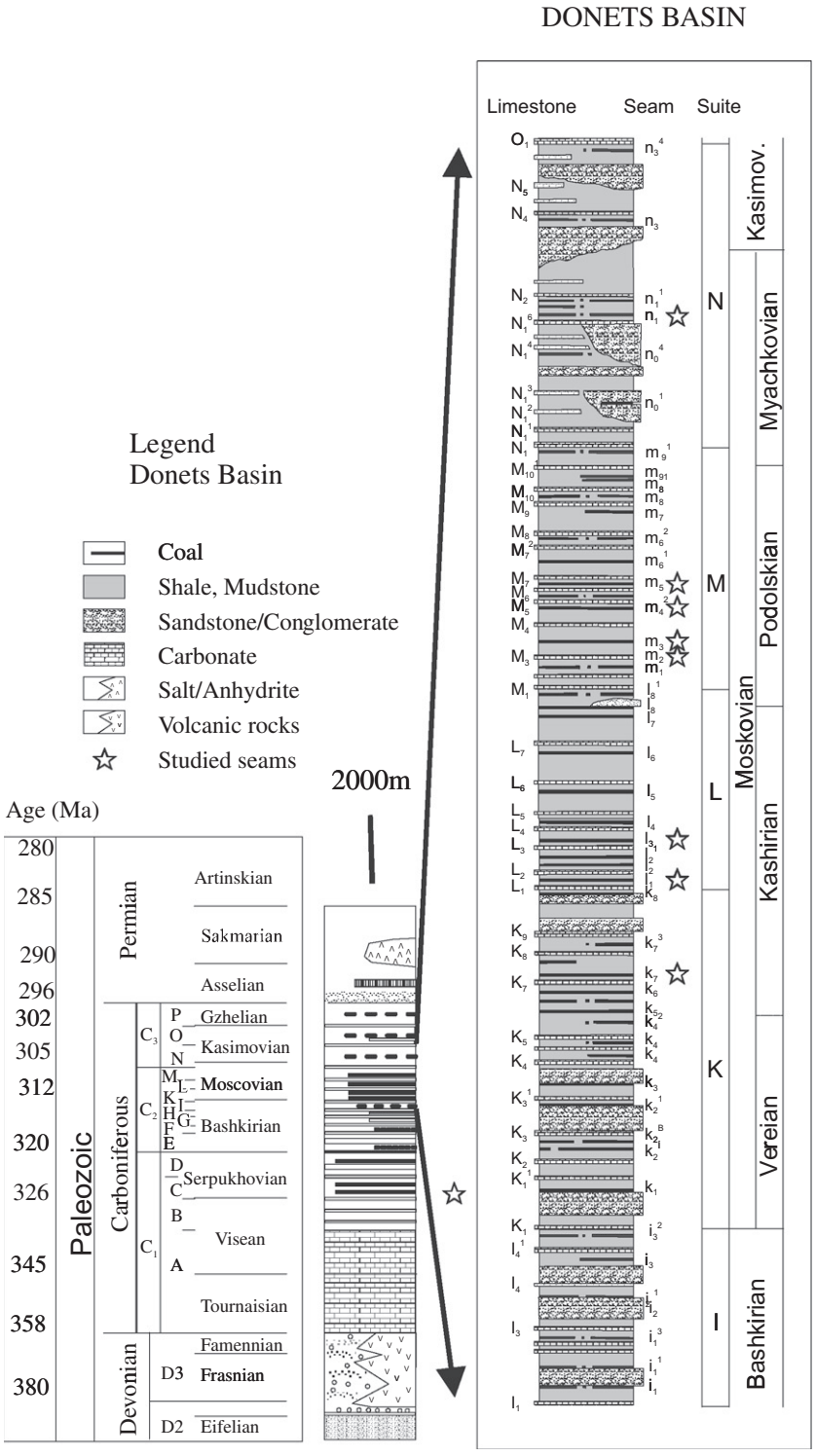

Fig. 4. Lithostratigraphic column from Donets Basin (modified after Izart et al. (2006)).

if necessary to correct the samples from H_2 reference gas drift in the dual-inlet. The uncertainty was estimated after three to five replicates. Total uncertainty was obtained after combining standard uncertainty ($\sigma_{standard}$) and peak uncertainty (σ_{peak}) according to the following equation:

$$\sigma_{tot.} = \sqrt{(\sigma_{standard})^2 + (\sigma_{peak})^2} \quad (1)$$

Here uncertainty is reported with 95% confidence limit on the basis of the uncertainty for both standard and peak (2σ).

3. OM type and maturity from Rock–Eval pyrolysis, organic petrography and molecular analysis

Three types of OM were identified (Fig. 10; Table 1) on the basis of the hydrogen index (HI), oxygen index (OI) and maximal temperature of the S2 peak (T_{max}) following the interpretations of Espitalié et al. (1985a,b, 1986) (Fig. 11):

(i) Samples with Type I (lacustrine) OM are characterized by HI > 800 mg/g as personified by the Green River oil shale

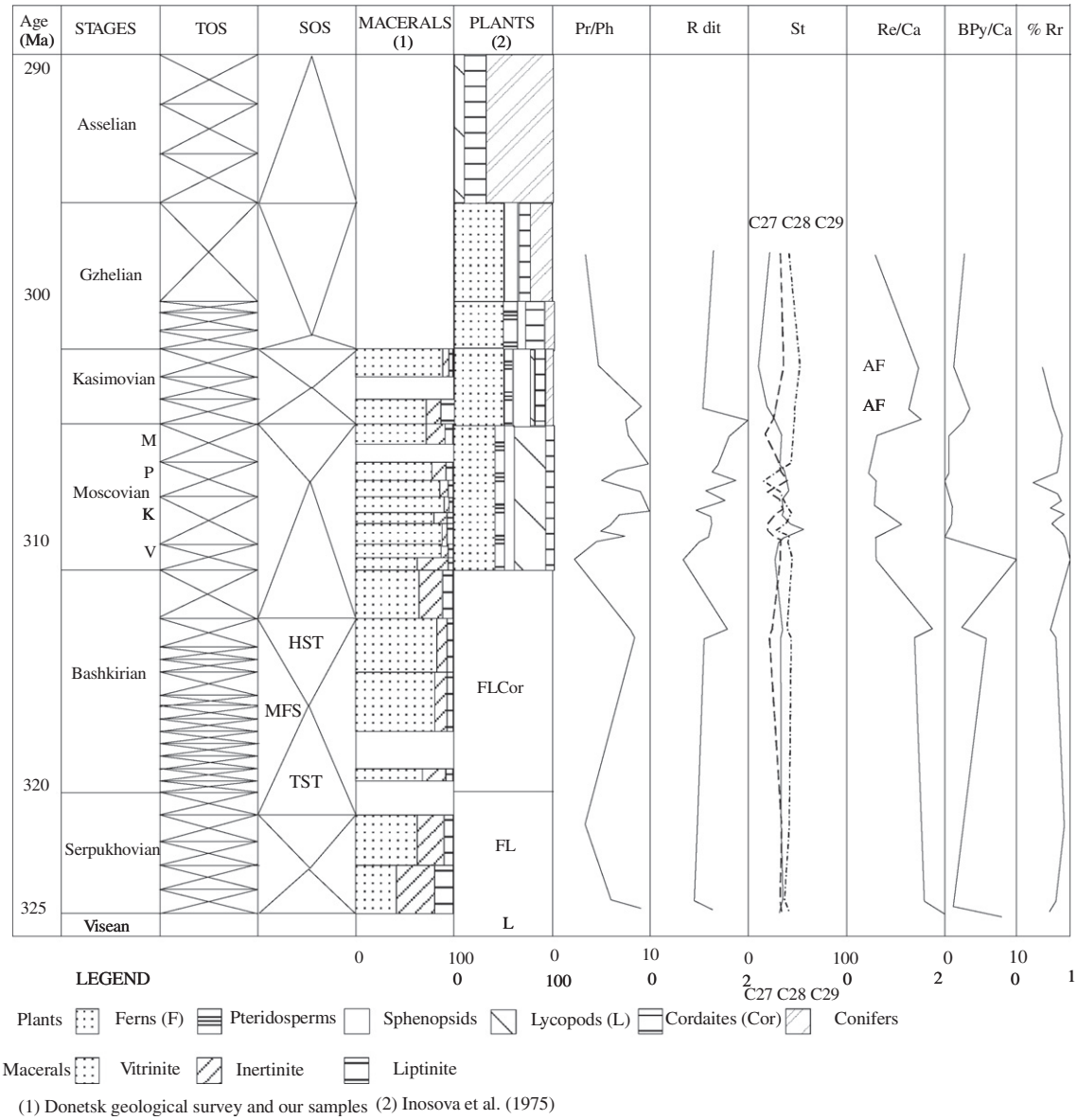

Fig. 5. Change in macerals of coals, plants and biomarkers in Donets Basin during Carboniferous and Early Permian (modified after Izart et al. (2006)). AF, arboranes/fernanes; BPy/Ca, benzopyrenes/cadalene; HST, highstand system tract; K, Kashirian; M, Myachkovian; MFS, maximum flooding surface; P, Podolskian; R_{dit}, diterpanes ratio; Re/Ca, retene/cadalene; % Rr, vitrinite reflectance; SOS, second order sequence; St: steranes; TOS, third order sequence; TST, transgressive system tract; V, Vereian. (See above-mentioned reference for further information.)

(USA) containing *Botryococcus braunii* (Espitalié et al., 1985a). However, except for the Autun sample, the lacustrine samples had HI values between 100 and 500 mg/g, intermediate between Type II (marine) and Type III (humic). Such values were observed by Meyers and Lallier-Vergès (1999) for lacustrine OM from the Late Quaternary and could be explained by way of a mixture of algal and higher plant OM in the lacustrine sediments and a mineral matrix effect. Buillit et al. (1997) described HI values between 100 and 300 mg/g for recent sediments from the Annecy Lake, with higher values correlating with algal blooms. Bechtel and Schubert (2009b) described values close to 120 mg/g during the maximum eutrophication in Lake Lugano and 50 mg/g in the oligotrophic Lake Brienz. OI values were low for the Autun, Saar and Buxieres samples, low and high for the Lodève samples and high for the Moscow samples. T_{max} values ranged from 420 to 452 °C and VRr from 0.4% to 0.8%, indicating an immature kerogen for the bogheads from the Moscow Basin (Wollenweber et al., 2006) and oil window maturity for the bituminous shales and bogheads from the Saar (Müller, 2007), Autun (Doubinger and Elsass, 1975) and Lodève (Schlepp et al., 2001) basins. The bogheads from the Autun and Moscow basins (Fig. 11A and B) contained 70% alginite completely composed of *Botryococcus*, 5% sporinite, 5% vitrinite, 5% inertinite and 15% mineral matter. The black shales from the Saar Basin (Müller, 2007) contained alginite, vitrinite, cutinite, inertinite and mineral matter.

(ii) Samples with Type III (humic coal) OM showed HI values from 100 to 300 mg/g and corresponded to coals from the Donets Basin with vitrinite (100–200 mg/g) and hydrogen-rich vitrinite (200–300 mg/g) and a high amount (%) of liptinite (Sachsenhofer et al., 2003; Izart et al., 2006; Alsaab et al., 2007). The OI values for the Donets coals were low. T_{max} values ranged from 420 to 470 °C and VRr varied from 0.5% to 1%, indicating a maturity from immature up to the beginning of the gas window. The Donets coals (Fig. 11C

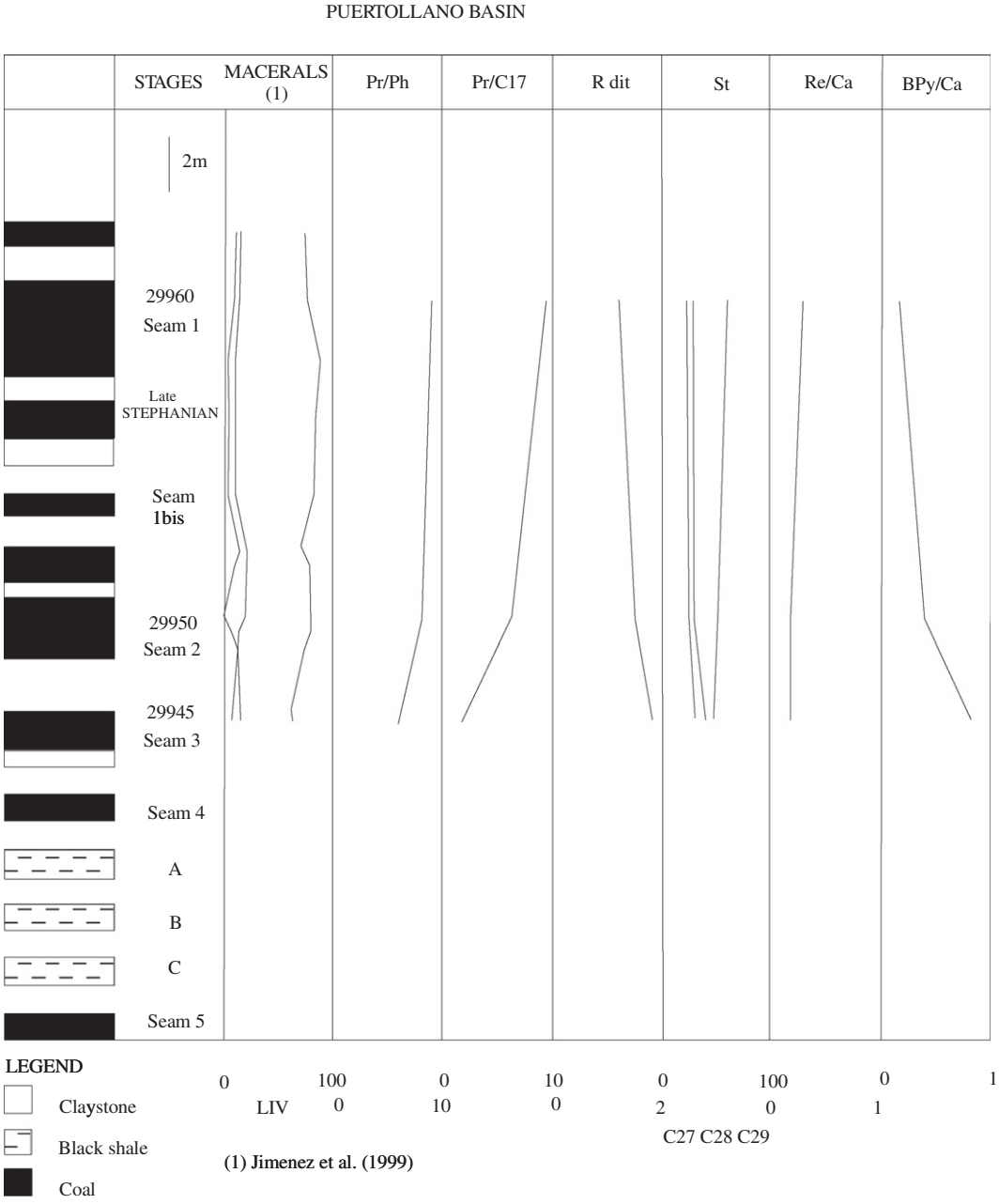

Fig. 6. Lithostratigraphical column with macerals and biomarkers from the Puertollano Basin (Jimenez et al., 1999). BPy/Ca, benzopyrenes/cadalene; Pr/Ph, pristane/phytane; R_{dit}, diterpanes ratio; Re/Ca, retene/cadalene; St, steranes.

and D) contained 56–92% vitrinite, 4–58% inertinite, 5–26% liptinite (mainly sporinite) and 1–20% minerals (Sachsenhofer et al., 2003; Izart et al., 2006). The BX3 coal contained 78% vitrinite and 22% liptinite (mainly sporinite) and VRr was 0.43%.

(iii) Samples with Type III (dispersed humic) OM were characterized by HI values <100 mg/g. The OI values were low and T_{max} values from 420 to 440 °C indicated a maturity from immature to the oil window for some bituminous shales from the Saar Basin (Müller, 2007).

Molecular analysis also allowed the OM maturity to be determined. Izart et al. (2006) discussed the maturity of the Donets coals. The *n*-alkanes, isoprenoids, hopanes and steranes were probably weakly influenced by maturity because of the generally low rank of the coals with VRr < 0.9%. For higher rank, Alsaab et al. (2007) demonstrated by pyrolysis of the Donets coals that the proportion of biomarkers changed. A decrease in 10% was observed for pristine/phytane (Pr/Ph) between VRr 0.6 and 1.

Hopane [$RC_{32}H = 22S/(22S + 22R)$], sterane [$RC_{29}S = 20S/(20S + 20R)$] and methyl phenanthrene (MPI-1) index values are listed and defined in Tables 2 and 3 and Fig. 12. For the Donets coals, Izart et al. (2006) showed that there were high volatility bituminous coals inside the oil window with $RC_{32}H$ and $RC_{29}S$ at the equilibrium values. Three samples were immature and two were at the beginning of gas window. The maximum values for $RC_{32}H$ and $RC_{29}S$ were close to 0.6% for VRr 0.6% and 0.8% (Fig. 12; Peters et al., 2005). A VR could also be calculated (VR_C) from MPI-1 and compared with the measured VRr value. Formulae for the relationship between VR_C and MPI-1 ($VR_C = 0.6 \times$

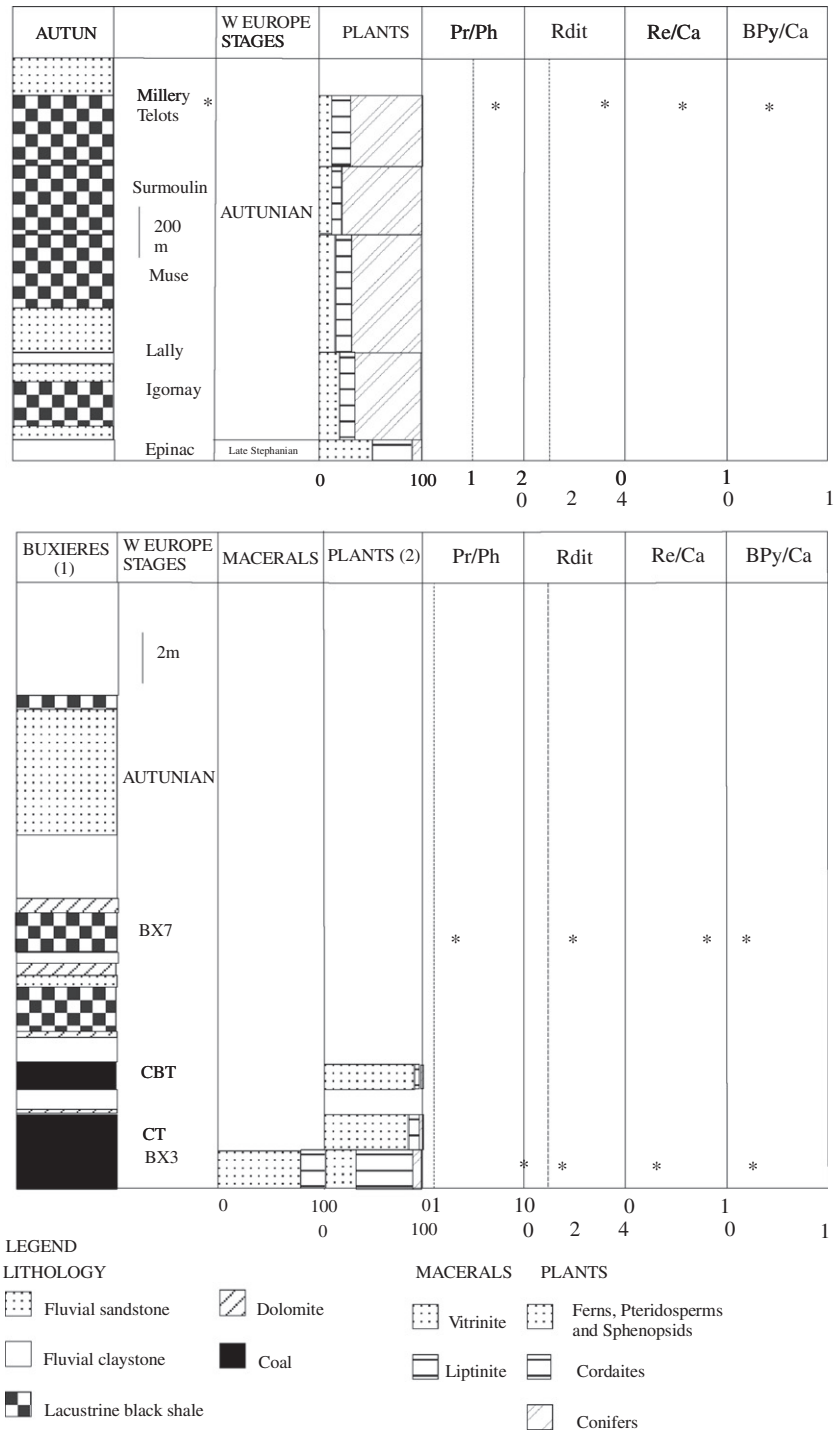

Fig. 7. Lithostratigraphic columns from Autun and Buxieres basins. For Autun Basin, the palynology is after Doubinger and Elsass (1975) and the organic geochemistry after Marteau (1983). For Buxieres Basin, the petrography is after Debriette (1992) and the palynology after Paquette et al. (1980). BPy/Ca, benzopyrenes/cadalene; Pr/Ph, pristane/phytane; R_{dit}, diterpanes ratio; Re/Ca, retene/cadalene.

MPI-1 + 0.4) established for the coals from the Ruhr Basin (Radke et al., 1982) correlated better with the Donets coals. The formulae ($VR_C = 0.6 \times MPI\text{-}1 + 0.24$) given by Radke et al. (2005) for the Permian and Jurassic marine deposits (Type II OM) correlated well with the lacustrine deposits (Type I OM), giving a similar thermal maturity as the other biomarkers.

The bogheads from the Moscow Basin had a lower maturity than other samples, with a VRr of 0.4% corresponding to brown coals (Wollenweber et al., 2006). T_{max} and biomarker ratios are also consistent with this maturity. The samples from the Puertollano, Autun, Buxieres and Saar basins have a VRr from 0.6% to 0.7% (Doubinger and Elsass, 1975; Müller, 2007 and our data) and are consistent with T_{max} and biomarker ratios for the oil window. These biomarkers were probably weakly influenced by maturity. T_{max} and RC_{32} hopane values were consistent with maturity in the oil window for the Lodève Basin samples (Schlepp et al., 2001).

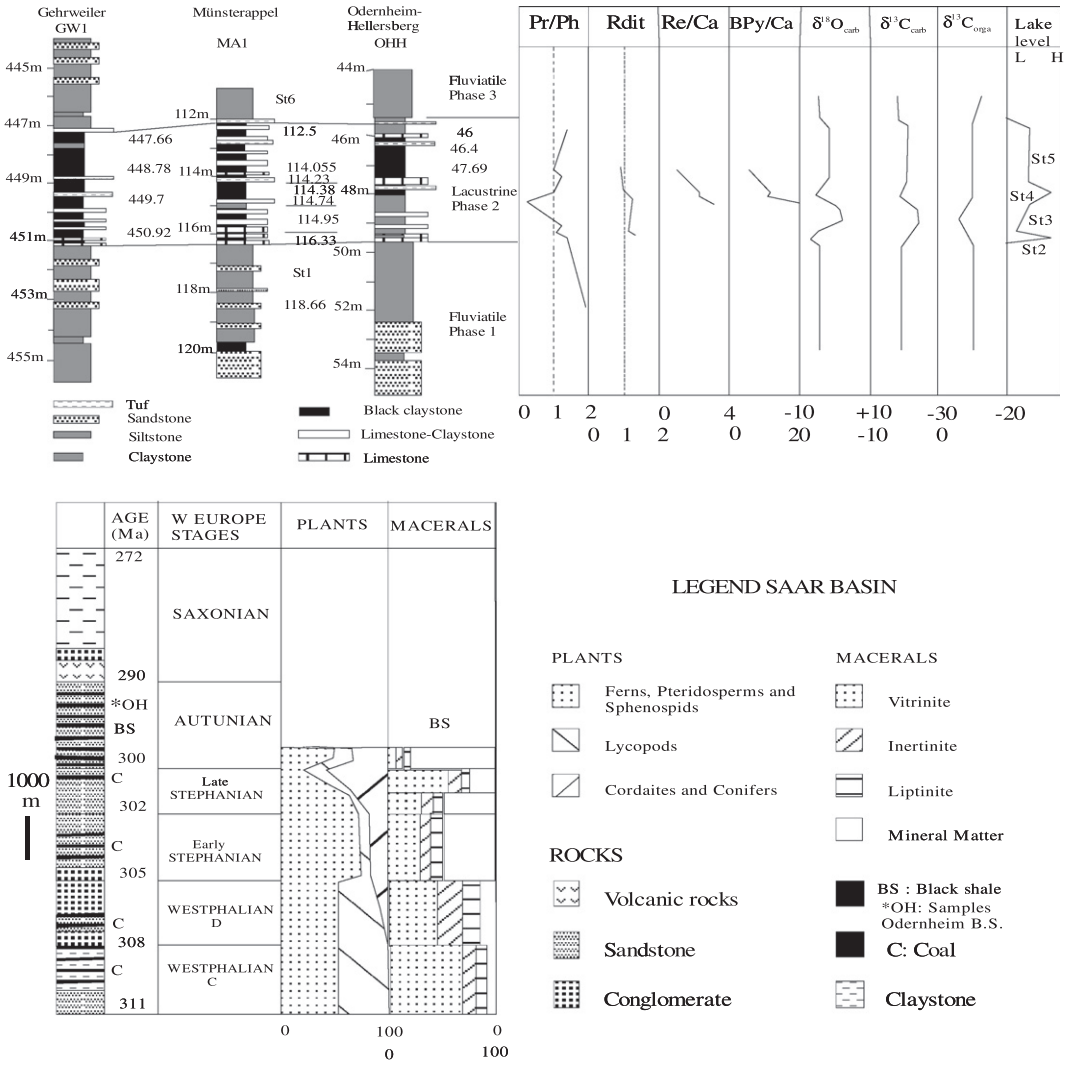

Fig. 8. Lithostratigraphic column with macerals and plants from the Saar Basin (Vliex et al., 1994) and lithostratigraphic column with the location of samples, biomarkers and phases of sedimentation in the Odernheim limnic black shale (Müller, 2007). BPy/Ca, benzopyrenes/cadalene; $\delta^{13}C_{carb}$, carbonate carbon isotopes values (‰ PDB; Müller, 2007); $\delta^{13}C_{orga}$, organic carbon isotopes values (‰ PDB; Müller, 2007); $\delta^{18}O_{carb}$, carbonate oxygen isotopes values (‰ PDB; Müller, 2007); H, high lake level; L, low lake level; Pr/Ph, pristane/phytane; R_{dit}, diterpanes ratio; Re/Ca, retene/cadalene; St, hydrological stage.

4. Molecular analysis and palaeoenvironmental interpretation

4.1. n-Alkanes and isoprenoids – sources of OM and conditions of preservation

Distributions of *n*-alkanes and isoprenoids reflect source inputs and the conditions of deposition and preservation of the OM. Two representative *n*-alkane and isoprenoid distributions are presented in Fig. 13. The humic coal samples from the Serpukhovian, Bashkirian, Moscovian, Kasimovian and Gzhelian of the Donets Basin (Sachsenhofer et al., 2003; Izart et al., 2006) contain a variable proportion (Table 1) of short chain (3–58% for C_{12}–C_{16} and 8–37% for C_{17}–C_{19}), a high proportion of mid-chain (16–40% for C_{20}–C_{24}) and a variable proportion of long chain *n*-alkanes (7–49% for C_{25}–C_{35}). The distributions are generally unimodal, with a maximum close to *n*-C_{17} (Fig. 13). The carbon preference index (CPI, Table 1) ranges from 1 to 1.6. The predominance of odd and long chain *n*-alkanes can be explained by the presence of higher plants, which is consistent with a swampy environment of deposition. The humic coal samples from the Stephanian (Puertollano) and Autunian (Buxieres) have unimodal or bimodal distributions with a maximum close to *n*-C_{17} and *n*-C_{28}, consistent with some Stephanian (Kasimovian) samples from the Donets Basin (o_2, $n_{3.6}$, $n_{3.2}$). The occurrence of long chain *n*-alkanes with an odd predominance is indicative of higher plants (Eglinton et al., 1962; Eglinton and Hamilton, 1967; Rieley et al., 1991). The occurrence of medium chain *n*-alkanes is known to be associated with *Sphagnum* in recent peat bogs, with a predominance of C_{23} and C_{25} (Bingham et al., 2010) and in submerged/floating aquatic plants in recent peat deposits and lake sediments (Yamamoto et al., 2010; Aichner et al., 2010a). Mid-chain *n*-alkanes also can be attributed to fire (Jaraula et al., 2010, 2011). The occurrence of short chain *n*-alkanes with an even predominance also is known for higher plants and soils from Australia under a semi-arid climate (Kuhn et al., 2010). For a swamp, there are many hypotheses to explain the presence of short and medium chain *n*-alkanes: high water level in the swamp with an algal bloom, the presence of *Sphagnum* and other mosses (*Muscites* is known during the Carboniferous) or higher plants that produced such *n*-alkanes. The origins of even and odd *n*-alkanes in plants have been studied by Zhou et al. (2010) who proposed different pathways for their biosynthesic precursors.

The boghead samples from the Viséan of the Moscow Basin and black shales from the Late Stephanian of the Puertollano Basin, the Autunian of the Buxieres Basin and Saar Basin (Odernheim black

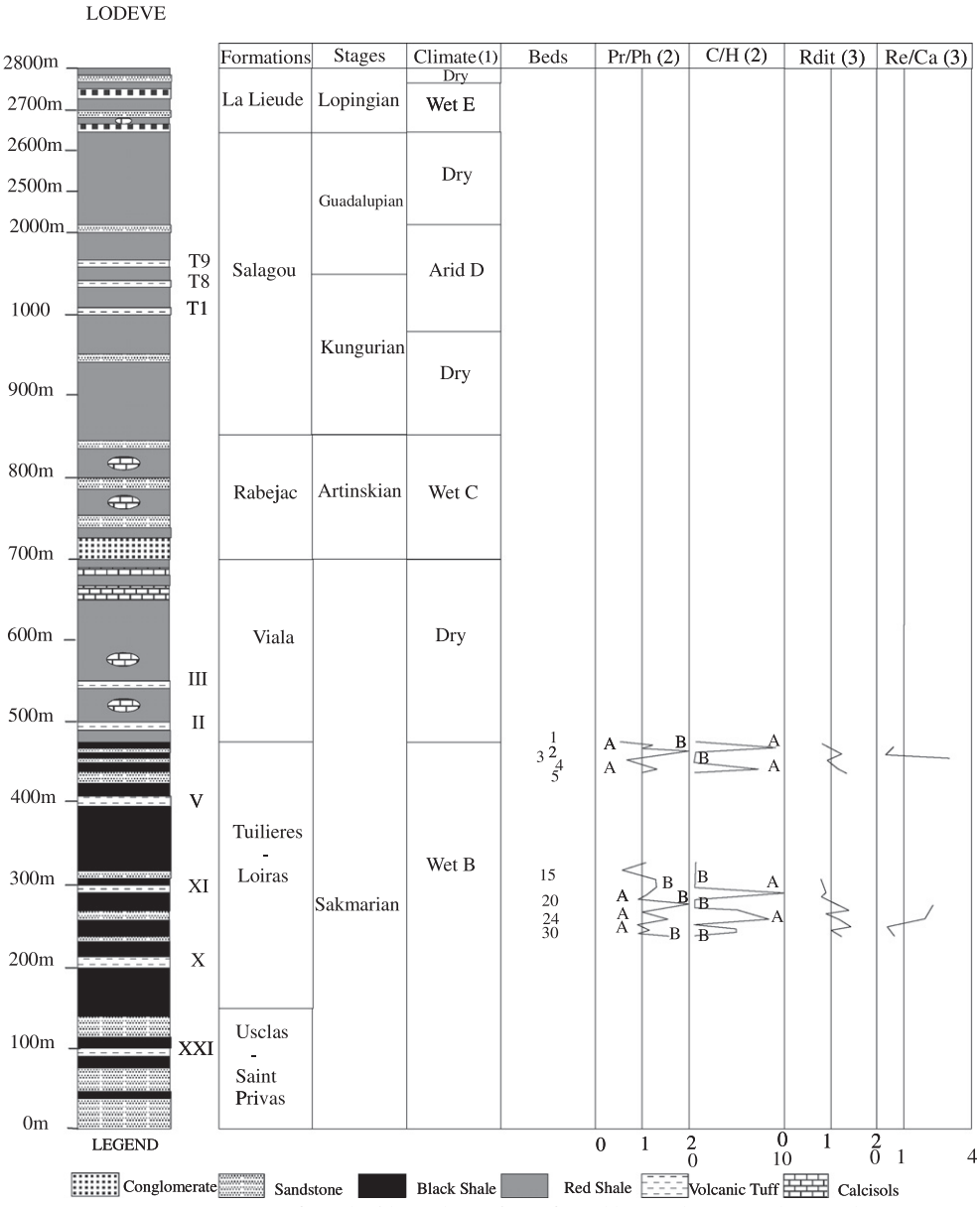

Fig. 9. Lithostratigraphic column from Lodève Basin with location of dry and wet periods (Schneider et al., 2006) and beds studied by Schlepp et al. (2001). A and B, groups A and B defined by Schlepp et al. (2001); C/H, cheilanthanes/hopanes; Pr/Ph, pristane/phytane; R_{dit}, diterpanes ratio; Re/Ca, retene/cadalene.

shales) and the Permian from the Lodève Basin have unimodal distributions with a maximum at *n*-C_{15} or bimodal distributions with maxima at *n*-C_{15} and *n*-C_{21} or *n*-C_{23} (Fig. 13). They contained a variable proportion of short chain (1–30% for C_{12}–C_{16} and 1–56% for C_{17}–C_{19}), mid-chain (3–45% for C_{20}–C_{24}) and long chain (7–95% for C_{25}–C_{35}) *n*-alkanes. The samples from the Autunian of Autun and Saar basins exhibited a similar abundance for each class, whereas those from the Viséan of the Moscow Basin have a predominance of long chain *n*-alkanes. CPI values (Table 1) range from 1 to 1.8, revealing a slight predominance of odd *n*-alkanes for the Moscow, Puertollano, Buxieres, Saar and Lodève samples. A CPI value of 0.9 revealed a slight predominance of even *n*-alkanes for the Autun sample. The predominance of odd long chain *n*-alkanes can be explained by the presence of higher plants. The predominance of even short chain *n*-alkanes can be explained by the presence of phytoplankton. These two cases are compatible with the types of OM in a lake, with a mixture of algae in the water column and higher plant material transported from the land. In recent lacustrine deposits, short and medium chain groups (C_{12}–C_{21}) are from algae, C_{22}–C_{26} probably from submerged plants and C_{27}–C_{35} from higher plants. A mixture of terrestrial humic and algal OM was observed for the Odernheim Lake, and submerged plants (Palaeochara) were reported during the Carboniferous and Permian. Ficken et al. (2000) and McKirdy et al. (2010) used the Paq ratio as $(C_{23} + C_{25})/(C_{23} + C_{25} + C_{29} + C_{31})$ to determinate the presence of terrestrial plants (<0.1), emergent aquatic plants (0.1–0.4) and non-emergent (submerged and floating leaves) plants (0.4–1). The ratio, ranging from 0.4 to 0.8 for our coals, bogheads and limnic shales, seems not to be valid for our samples.

B. braunii is known to be present in the Autun and Moscow bogheads and Puertollano and Odernheim black shales, but only the Autun and Odernheim samples had a predominance of short chain *n*-alkanes. These *n*-alkanes were observed by Derenne et al. (1994), Han et al. (1995, 1999) and Han and Kruge (1999) in boghead coals.

Table 2
Biomarker and mean δD data.[a]

Sample	Locality	Lithology	R_{dit}	C_{27}	C_{28}	C_{29}	$C_{27/29}$	RC_{29}	H/S	RC_{32}	$C_{29/30}$	$C_{35/34}$	$C_{22/21}$	$C_{24/23}$	C/H	G	MPI1	VR_C	Re/Ca	BP/Ca	Ar/Ca	δDC_{16-21}	$\delta D\ C_{22-26}$	$\delta D\ C_{27-35}$
LC1A	Lodeve	LBS	0.85	33	23	44	0.75	0.47		0.58	0.7	0.57		0.62	0.2	1.9	0.8	0.72	0.54	0.24				
LC3A	Lodeve	LBS	0.96								0.85	0.82	0.1	0.66	0.84	2.3			2.9	0.2				
LC4	Lodeve	LBS	1.05	15	28	56	0.27	0.5		0.52	0.68	0.48	0.22	0.7	7.38	0								
LC17A	Lodeve	LBS	0.87	29	25	46	0.63	0.53		0.58	0.73			0.46	0.11	1.5								
LC23A	Lodeve	LBS	1.27	11	27	62	0.18	0.5		0.52	1.38	0.25	0.3	0.59	5.91	0	0.62	0.61						
LC24A	Lodeve	LBS	1.12	15	29	56	0.27	0.49		0.5	0.73	0.76		0.59	8.9	1.3	0.48	0.53	2.2	0.41				
LC28	Lodeve	LBS	0.97								0.55		0.24	0.72	5.4	0								
LC30A	Lodeve	LBS	1.13	19	36	45	0.42	0.53		0.6	0.73	0.29	0.24	0.63	5.2	0	0.64	0.62	0.55	0.38				
MA1112.5	Münster	LBS																						
MA1114.0	Münster	LBS	0.79	34	29	37	0.9	0.59	10	0.59	0.4		1.07	5.02	0.2	4.45	0.66	0.64	1.14	6	0			
MA1 114.23	Münster	LBS																						
MA1 114.38	Münster	LBS	0.84	32	32	36	0.9	0.6	6	0.6	0.44		1.35	4.58	0.37	4.65	0.63	0.62	2.2	10.8	0			
MA1114.74	Münster	LBS	1.05	33	34	33	1	0.6	8	0.6	0.33		1.52	5.81	0.27	4.9	0.64	0.62	2.2	9.8	0			
MA1114.95	Münster	LBS																				-98.67	-84.45	-104.59
MA1116.33	Münster	LBS	1.17	31	28	41	0.8	0.6	2	0.58	0.69		1.16	4.36	1.05	4.46								
MA1118.66	Münster	LBS																						
GW1449.70	Gehrweiler	LBS	0.96	29	28	43	0.7	0.6	6	0.54	0.39		2.27	4.72	0.52	5.2	0.53	0.56	3.2	21	0			
GW1450.9	Gehnwiler	LBS																				-108.66	-93.47	-81.84
OH46.01	Odernheim	LBS	0.95	33	29	38	0.9	0.6	11	0.59	0.31		1.86	6.56	0.16	3.97	0.66	0.64	1.3	6	0			
OH46.40	Odernheim	LBS																						
OH47.69	Odernheim	LBS																				-99.32	-88.98	-80.95
AU1	Autun	BC	3.2	21	48	31	0.68	0.45	1.73	0.54	1	0.51	0.09	0.19	1.14	1.82	0.51	0.55	0.6	0.48	1.87	-67.25	-55.36	-41.35
BX3	Buxieres	HC	1.5	17	32	51	0.33	0.37	9.33	0.58	0.56	0.5					0.61	0.6	0.29	0.22	1.51			
BX7	Buxieres	LBS	2	31	23	46	0.67	0.39	18.2	0.58	0.67	0.85					0.77	0.7	0.85	0.16	5.42			
P 29960	Puertollano	HC	1.14	23	24	53	0.45	0.2	11.9	0.48							0.39	0.63	0.28	0.17	0.15			
P 29950	Puertollano	HC	1.55	26	25	49	0.52	0.2	10	0.47							0.51	0.75	0.16	0.42	0.35			
P 29945	Puertollano	HC	1.9	28	33	39	0.7	0.2	7	0.5							0.32	0.68	0.17	0.8	0.19			
PB	Puertollano	LBS		40	30	30	1.33																	
p5 Lug	Donets	HC	1.3	24	34	42	0.57	0.52	15.3	0.59							0.48	0.69	0.5	3	0.16	-144.2		-77.8
o2 Svet	Donets	HC	1.1	12	37	51	0.23	0.16	11.1	0.26							0.16	0.5	1.42	1	3.28			
H36MC	Donets	HC	1	24	28	48	0.5	0.37	12	0.57							0.56	0.74	1.18	2.87	4.33			
H23MC	Donets	HC	2.2	25	25	50	0.5	0.4	10	0.57							0.42	0.65	1.66	1.9	0.23			
H22MC	Donets	HC	2.2	19	28	53	0.36										0.37	0.62						
5nlBnt	Donets	HC	1.1	38	15	47	0.81	0.56	18.4	0.6							0.32	0.59	0.51	0.25	0			
4n1But	Donets	HC	1.5	28	24	48	0.58	0.6	21.5	0.6							0.6	0.76	0.57	1.78	0			
3n1But	Donets	HC	1.6	31	23	46	0.67	0.6	20.8	0.6							0.53	0.72	0.74	0.14	0			
2n1But	Donets	HC	2	25	26	49	0.51	0.6	22.3	0.59							0.62	0.77	0.04	0.45	0			
1n1But	Donets	HC	1.7	26	28	46	0.56	0.6	17.7	0.59							0.6	0.76	0.25	0.41	0	-114.5		-110.1
m3Trado	Donets	HC	1.7	42	42	16	2.62	0.21	0.5	0.27							0.52	0.71	0.32	0.37	0			
m2Bel	Donets	HC	1.2	45	22	33	1.36	0.6	11.5	0.62							0.62	0.77	0.46	0	0			
l4 Trudo	Donets	HC	1	30	33	37	0.81	0.19	9.5	0.47							0.23	0.54	0.38	0.06	0			
9l1 Dim	Donets	HC	1.2	47	25	28	1.68	0.6	8.1	0.6							0.33	0.6	1.04	0.18	0			
8l1 Dim	Donets	HC	1.2	43	25	32	1.34	0.6	9	0.59							0.29	0.57	1.14	0.07	0			
6l1 Dim	Donets	HC	1.2	41	26	33	1.24	0.6	9.2	0.59							0.3	0.58	2.16	0.06	0			
5l1 Dim	Donets	HC	1	38	16	46	0.82	0.6	14.6	0.59							0.32	0.59	0.96	0.08	0			
4l1 Dim	Donets	HC	1.2	36	31	33	1.09	0.6	9	0.59							0.3	0.58	0.97	0.05	0			
3l1 Dim	Donets	HC	1.2	42	16	42	1	0.6	14.7	0.58							0.34	0.6	0.74	0.05	0			
2l1 Dim	Donets	HC	1.1	43	21	36	1.19	0.58	13	0.6							0.32	0.59	0.99	0.05	0			
1l1 Dim	Donets	HC	1.4	42	16	42	1	0.59	14.3	0.6							0.28	0.57	0.38	0.05	0	-101.7	-86.4	-75.25
1k8 Nov	Donets	HC	1.2	56	19	25	2.24	0.6	6.3	0.6							0.3	0.58	0.52	0	0			
2 k22 Ka	Donets	HC	0.7	30	28	42	0.71	0.53	1.3	0.6							1.03	1.02	0.31	6.19	0			
lk22Ka	Donets	HC	0.7	24	27	49	0.49	0.6	1.1	0.6							1.1	1.06	0.64	14.5	0			
3hlOPe	Donets	HC	1.6	39	26	35	1.11	0.58	11.2	0.59							0.32	0.59	1.76	1.81	0			
2hlOPe	Donets	HC	1.3	33	25	42	0.78	0.6	17.9	0.59							0.32	0.59	1.42	5.41	0	-107.33	-60.5	-69.86
dl YD	Donets	HC	1	37	29	34	1.09	0.52	17.5	0.6							0.51	0.71	1.59	0.24	0			

Table 2 (*continued*)

Sample	Locality	Lithology	R_{dit}	C_{27}	C_{28}	C_{29}	$C_{27/29}$	RC_{29}	H/S	RC_{32}	$C_{29/30}$	$C_{35/34}$	$C_{22/21}$	$C_{24/23}$	C/H	G	MPI1	VR_C	Re/Ca	BP/Ca	Ar/Ca	δDC_{16-21}	$\delta D\ C_{22-26}$	$\delta D\ C_{27-35}$
2 dO YD	Donets	HC	1.1	19	32	49	0.38										0.35	0.55	8.94	7.06	0			
IclOYD	Donets	HC	0.4	30	31	39	0.77	0.41	30.6	0.6							0.54	0.72	0.93	0	0			
4525 a	Moscow	BC	1.75	14	31	55	0.25	0.11	6.22	0.16	0.92	2.48	0.31	0.93	0.12	6.09	0.2	0.36	0.25	0.79	0			
4525 b	Moscow	BC	1.78	19	17	64	0.29	0.12	5.95	0.17	0.9	2.35	0.61	0.43	0.14	5.96	0.2	0.36	0.85	3.79	0			
E48985	Moscow	BC																	2.4		0			
E48986	Moscow	BC		28	34	38	0.74										0.25	0.39	0.6		0			
E48987	Moscow	BC		30	29	41	0.73										0.31	0.43	15		0			
E48988	Moscow	BC		27	37	36	0.75										0.57	0.58			0			
E48989	Moscow	BC		15	19	66	0.22										0.21	0.37	0.4		0			

[a] Ar/Ca, arboranes/cadalene; BC, boghead coal; BP/Ca, benzopyrenes/cadalene; C/H, cheilanthanes/hopanes; *C22/21* and *C24/23*, cheilanthane ratios; C_{27}, C_{28} and C_{29}, C_{27}, C_{28} and C_{29} steranes %; $C_{29/30}$, C_{29}/C_{30} hopanes; $C_{35/34}$, C_{35}/C_{34} hopanes; G, gammacerane ratio; H, hopanes; HC, humic coal; H/S, hopanes/steranes; LBS, lacustrine black shale; MPI1, methylphenanthrene index; S, steranes; RC_{32}, C_{32} hopanes ratio; RC_{29}, C_{29} steranes ratio; R_{dit}, diterpane ratio; Re/Ca, retene/cadalene; VR_C, vitrinite reflectance calculated from MPI-1 (%) after formulae from Radke et al. (1982) for Carboniferous coals from Ruhr Basin and Radke et al. (2005) for marine Jurassic and Permian shales.

Audino et al. (2001a,b) and Grice et al. (2001) found respectively macrocyclic alkanes and their methylated homologues, and monomethyl alkanes in the *Botryococcus*-rich bogheads from the Carboniferous of Scotland and from the Permian of South Africa and Australia. These compounds were not found in our bogheads. No botryococcane and lycopane were found in our bogheads that contained *B. braunii*. These compounds are known in recent and Tertiary sediments and oils, but have never been found in sediments from the Carboniferous and the Permian torbanites of Australia, South Africa, Scotland and Autun (Derenne et al., 1994; Grice et al., 2001; Audino et al., 2002; Zhang et al., 2007).

A plot of Pr/*n*-C_{17} vs. Ph/*n*-C_{18} (Fig. 14) shows that the ratios were higher for the coals deposited under swampy conditions than those for the claystone deposited in lakes. Peters et al. (2005) defined different fields for such a diagram: Type III, Type II and intermediary domain. From this interpretation, the conditions of deposition of lacustrine shale are more reduced and of a swampy coal more oxidized if it was located at the peat surface. Type I, not located in the diagram of Peters et al. (2005), is located between Type II (marine) and Type III (terrestrial higher plant) OM after our lacustrine samples. These intermediate types can be explained by the presence of algae and higher plants in the lacustrine deposits, whereas algae predominated in sample MA1 114.735, which represents a Type II kerogen. In the diagram, the diverse stages defined by Müller (2007) could be differentiated: fluvial stage 1 (Type III OM), underbalanced lacustrine stage 3 with evaporation > input of water (intermediate type OM), balanced lacustrine stages 2 and 5 with evaporation equal to input of water (intermediate type OM) and overbalanced lacustrine stage 4 with evaporation < input of water (Type I OM with algae equivalent to Type II). The Pr/Ph values (Table 1) showed that the conditions of oxidation were higher for the coals than the lacustrine black shales. Three groups could be defined: (i) Pr/Ph < 1 for Moscow bogheads and black shales from Saar (SA4) and Lodève (Fig. 9, group A from Schlepp et al. (2001)); (ii) 1 < Pr/Ph < 3 for Moscow and Autun bogheads, black shales from Saar (SA2 and SA5), Puertollano, Buxieres and Lodève (Fig. 9, group B from Schlepp et al. (2001)); (iii) Pr/Ph > 3 for Donets, Buxieres and Puertollano humic coals. Fig. 14 and Pr/Ph allowed us to differentiate swamp and lake deposits from the type of OM deposited under an oxidizing or reducing environment.

4.2. Terpanoid hydrocarbons and steranes – sources of OM and conditions of preservation

Saturated biomarkers are standard tools in characterizing sedimentary OM. Two hopane distributions are presented in Fig. 13. All the samples showed similar patterns, characterized by a dominance of the C_{30} hopane. The hopanes/steranes ratio was high in the humic coal samples from the Donets Basin, ranging from 0.5 to 38 with a mean of 13.3 (Table 2, Fig. 5). The ratio was variable for bogheads (6 for Moscow samples and 1.9 for Autun sample) and high (2–18) for black shales and humic coals from the Autunian Buxieres and Saar basins and Late Stephanian Puertollano Basin. High values suggest intense reworking and high bacterial input (Ourisson et al., 1979, 1984). Derenne et al. (1998) also observed high values (17–43) for torbanites from the Permian of Australia and South Africa.

A plot (Fig. 15) of C_{35}/C_{34} 22*S* homohopanes vs. norhopane/hopane (C_{29}/C_{30}) can be used to define source facies (Peters et al., 2005). Most oils from reduced marine carbonate source rocks show high C_{35}/C_{34} values (>0.8) combined with high C_{29}/C_{30} values (>0.6), and oils from oxic coal/resin and lacustrine source rocks show lower values. Black shales from the Saar and Lodève basins exhibited low C_{29}/C_{30} and C_{35}/C_{34} values, consistent with lacustrine deposits, and the boghead from the Moscow Basin had high C_{29}/C_{30}

and C_{35}/C_{34} values, consistent with marine deposits. As this coal is located under marine limestone, the water was perhaps brackish. The boghead from the Autun Basin showed high C_{29}/C_{30} and low C_{35}/C_{34} values.

The distribution of tricyclic terpanes (cheilanthanes, Fig. 13) is also indicative of source facies (Peters et al., 2005). Marine shale source rocks contain high C_{24}/C_{23} and low C_{22}/C_{21} values, and marine limestone and lacustrine source rocks high C_{22}/C_{21} and low C_{24}/C_{23} values. A plot of C_{24}/C_{23} vs. C_{22}/C_{21} (Fig. 16) showed that the lacustrine black shales from the Saar Basin exhibited high values for the two ratios, and bogheads from the Autun and Moscow basins and black shales from the Lodève Basin low values. No cheilanthanes were detected in the coals. Cheilanthanes are derived primarily from algal or bacterial sources (Kruge et al., 1990; Revill et al., 1994; Nabbefeld et al., 2010b). The cheilanthanes/hopanes (C/H) ratio is low for Moscow, Saar and Lodeve (group B, Fig. 9) samples and high for the sample MA 116.3 from the Saar Basin (stage 2 of deposition) and the Autun and Lodeve (group A, Fig. 9) samples. A decametre-thick sequence corresponding to a high frequency sequence from the Lodeve Basin exhibited from base to top (Fig. 9): fluvial sandstone and then black shales with low C/H values (group B), then high C/H (group A) and finally low C/H (group B). These changes were explained by Schlepp et al. (2001) by way of an alternation of fresh water (group A)

Table 3
Peak assignments in chromatograms and formula for calculation of ratio.

Peak	Assignment	C_{no}
Diterpanes (m/z = 123)		
1	Labdane	
2	19-Norisopimarane	
3	*ent*-Beyerane	
4	*iso*-Pimarane	
5	16β-Phyllocladane	
6	16α-Kaurane	
7	16α-Phyllocladane	
8	16|3-Kaurane	
R_{dit} = (2 + 4 + 6)/(3 + 5 + 7)		
Steranes (m/z = 217)		
1	14α(H), 17α(H) – cholestane (20S)	C_{27}
2	14β(H), 17β(H) – cholestane (20R)	C_{27}
3	14β(H), 17β(H) – cholestane (20S)	C_{27}
4	14α(H), 17α(H) – cholestane (20R)	C_{27}
5	24-Methyl-14α(H), 17α(H) – cholestane (20S)	C_{28}
6	24-Methyl-14β(H), 17β(H) – cholestane (20R)	C_{28}
7	24-Methyl-14β(H), 17β(H) – cholestane (20S)	C_{28}
8	24-Methyl-14aαH), 17α(H) – cholestane (20R)	C_{28}
9	24-Ethyl-14α(H), 17α(H) – cholestane (20S)	C_{29}
10	24-Ethyl-14β(H), 17β(H) – cholestane (20R)	C_{29}
11	24-Ethyl-14β(H), 17β(H) – cholestane (20S)	C_{29}
12	24-Ethyl-14α(H), 17α(H) – cholestane (20R)	C_{29}
Hopanes (m/z = 191)		
1	18α(H)-22, 29, 30-trisnomeohopane (Ts)	C_{27}
2	17α(H)-22, 29, 30-trisnorhopane (Tm)	C_{27}
3	17β(H)-22, 29, 30-trisnorhopane	C_{27}
4	17α(H), 2ip(H)-30 norhopane	C_{29}
5	hop-17(21)-ene	C_{30}
6	17β(H)-21 α(H)-normoretane	C_{29}
7	17α(H), 2ip(H)-hopane	C_{30}
8	neohop-13(18)-ene	C_{30}
9	17β(H)-2ip(H)-30-norhopane + 17β(H)-21α(H)-moretane	$C_{29} + C_{30}$
10	17α(H), 21β(H) – 30 homohopane (22S)	C_{31}
11	17α(H), 21β(H) – 30 homohopane (22R)	C_{31}
12	17β(H)-2ip(H)-hopane	C_{30}
G	Gammacerane	C_{30}
13	17α(H), 21β(H) – 30 bishomohopane (22S)	C_{32}
14	17α(H), 21β(H) – 30 bishomohopane (22R)	C_{32}
Aromatics		
1	Naphthalene (m/z = 128)	
2	Methyl-naphthalene (m/z = 142)	
3	Dimethyl-naphthalene (m/z = 156)	
4	Trimethyl-naphthalene (m/z = 170)	
5	Cadalene (m/z = 183)	
6	Dibenzothiophene (m/z = 184)	
7	Phenanthrene (m/z = 178)	
8	Methyl-phenanthrenes (m/z = 192)	
9	Dimethyl-phenanthrene (m/z = 206)	
10	Pyrene (m/z = 178)	
11	Retene (m/z = 219)	
12	Chrysene (m/z = 228)	
13	Benzofluoranthene (m/z = 252)	
14	Benzo[a + e]pyrenes (m/z = 252)	
15	MATH (m/z = 393, 255)	
16	MAPH (m/z = 377, 239)	
17	DAPH1 (m/z = 374, 221)	
MPI1 = 1.5(2-MP + 3-MP)/(P + 1-MP + 9-MP)		

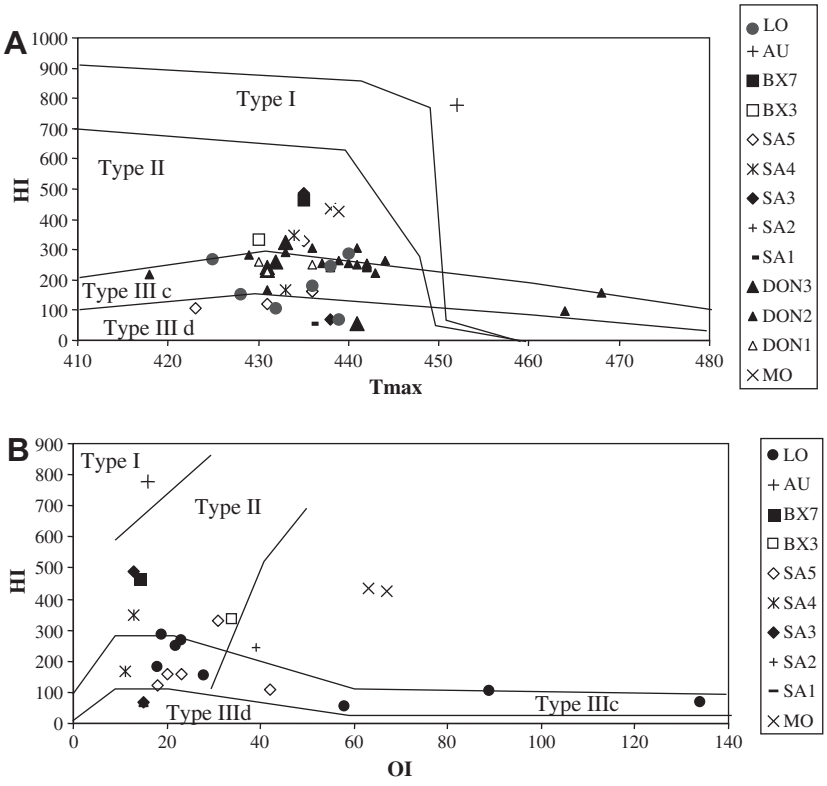

Fig. 10. Rock–Eval data. A: HI (mg/g TOC) vs. T_{max} (°C) and B: HI (mg/g TOC) vs. OI (mg/g TOC) for humic coals and lacustrine deposits. AU, Late Autunian boghead from Autun; BX3 and BX7, Early Autunian coal and black shale from Buxieres; DON 1 + 2 + 3, humic coals from Donets (respectively Serpukhovian, Bashkirian and Moscovian, Kasimovian and Gzhelian); LO, Lodève black shales; MO, Viséan bogheads from Moscow Basin; PB and PU, Late Stephanian black shale and humic coals from Puertollano. The Odernheim black shale samples (SA, Autunian from Saar) were labelled after the hydrological stages described by Müller (2007; see our Fig. 8): stage 1, fluvial; stages 2 and 5, evaporation = input of water to lake; stage 3, evaporation > input of water to lake; stage 4, evaporation < input to water in lake. Type I OM, lacustrine OM; Type II OM, marine OM; Type IIId OM, dispersed humic OM; Type IIIc, coal humic OM (after Espitalié et al. (1985a,b, 1986)).

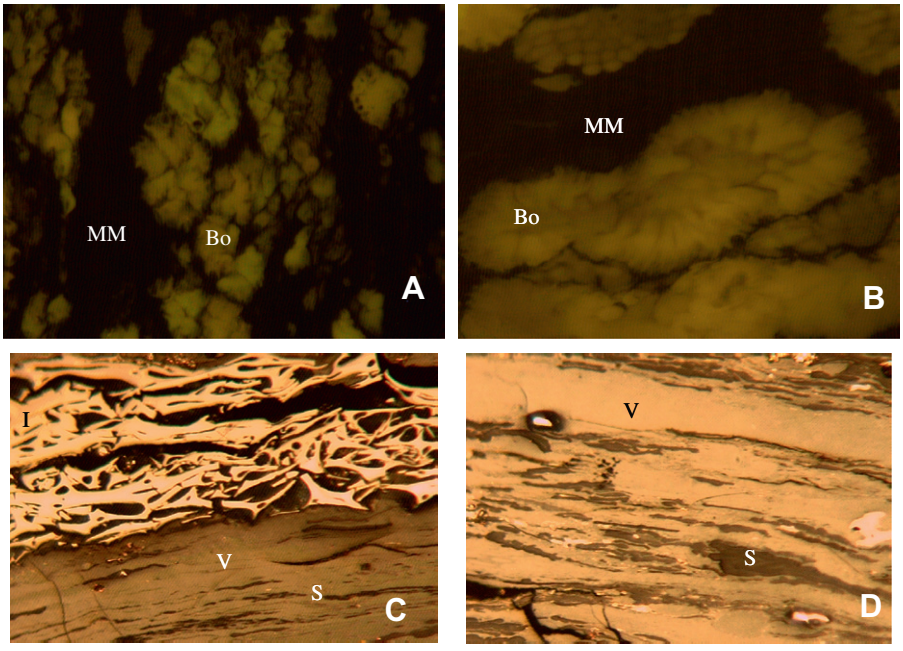

Fig. 11. Photographs of bogheads from Autun and Moscow basins, and Donets humic coals. A, Viséan boghead (sample 4225b) from Moscow; B, Autunian boghead from Autun; C and D, Moscovian l1Dim humic coal from Donets. Bo, *Botryococcus*; I, inertinite; MM, mineral matter; S, sporinite; V, vitrinite. The width of the thin sections is 200 μm.

and marine water (group B). Yawanarajah et al. (1993) proposed the same interpretation for the Permian black shales from Sudetes in Poland. However, sediments from the Lodève Basin contained no evidence for marine conditions. Another possibility would be the

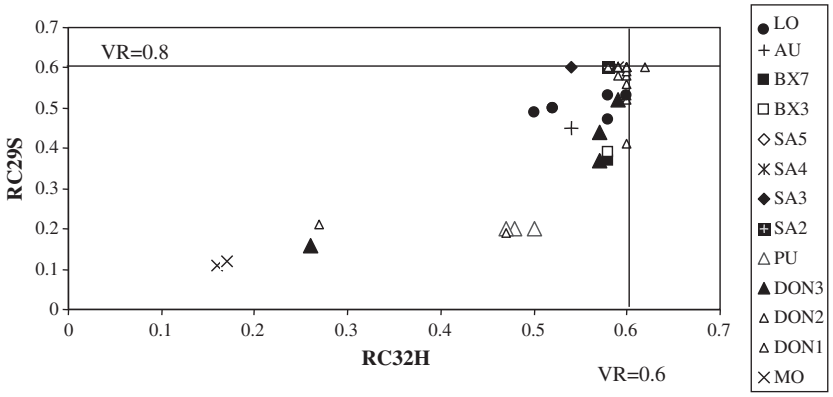

Fig. 12. RC_{29} steranes (RC_{29}S) vs. RC_{32} hopanes (RC_{32}H). AU, Late Autunian boghead from Autun; BX3 and BX7, Early Autunian coal and black shale from Buxieres; DON 1 + 2 + 3, humic coals from Donets (respectively Serpukhovian, Bashkirian and Moscovian, Kasimovian and Gzhelian); LO, Lodève black shales; MO, Viséan bogheads from Moscow Basin; PU, Late Stephanian humic coals from Puertollano. The samples from the Odernheim black shale (SA, Autunian from Saar) were labelled after the hydrological stages described by Müller (2007; see our Fig. 8). VR, vitrinite reflectance.

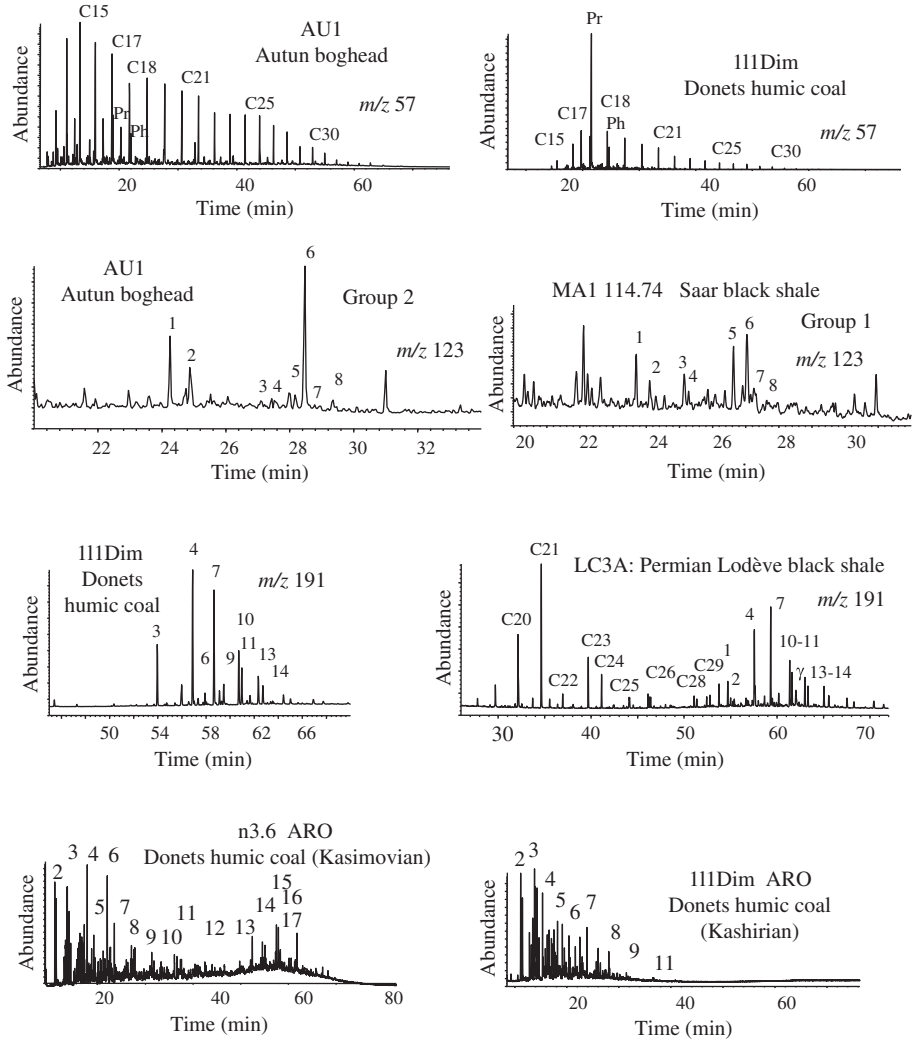

Fig. 13. Examples of *n*-alkane (*m*/*z* 57), diterpane (*m*/*z* 123), hopane (*m*/*z* 191) and aromatic (ARO) distributions from humic coals, bogheads and lacustrine deposits. Peaks are identified in Table 3.

formation of algal and bacterial blooms during the deposition of group A, linked with a period of maximum eutrophication, as observed for Lake Lugano (Bechtel and Schubert, 2009a,b).

Gammacerane was only observed in black shales from the Saar and Lodève (only group B) basins and bogheads from the Autun and Moscow basins. It is known to reflect stratification of the water

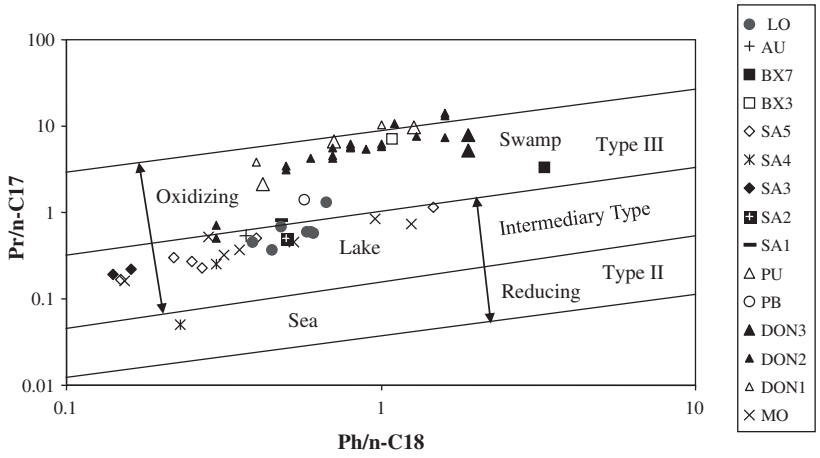

Fig. 14. Pr/n-C_{17} vs. Ph/n-C_{18} for humic coals and lacustrine deposits. AU, Late Autunian boghead from Autun; BX3 and BX7, Early Autunian coal and black shale from Buxieres; DON 1 + 2 + 3, humic coals from Donets (respectively Serpukhovian, Bashkirian and Moscovian, Kasimovian and Gzhelian); LO, Lodève black shales; MO, Viséan bogheads from Moscow Basin; PB and PU, Late Stephanian black shale and humic coals from Puertollano. The samples from the Odernheim black shale (SA, Autunian from Saar) were labelled after hydrological stages described by Müller (2007; see our Fig. 8): stage 1, fluvial; stages 2 and 5, evaporation = input of water to lake; stage 3, evaporation > input to water in lake; stage 4, evaporation < input to water in lake.

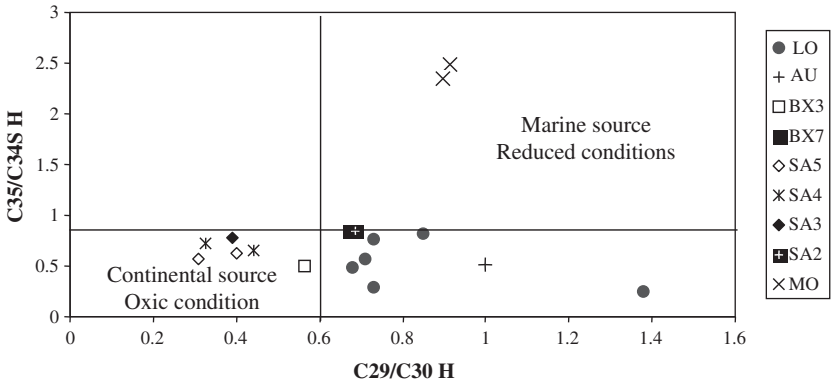

Fig. 15. C_{35}/C_{34} homohopanes (22S) vs. C_{29} (norhopane)/C_{30} (hopane). AU, Late Autunian boghead from Autun; BX3 and BX7, Early Autunian coal and black shale from Buxieres; LO, Lodève black shales; MO, Viséan bogheads from Moscow Basin; SA, samples from Odernheim black shale (Autunian from Saar) labelled after hydrological stages described by Müller (2007; see our Fig. 8).

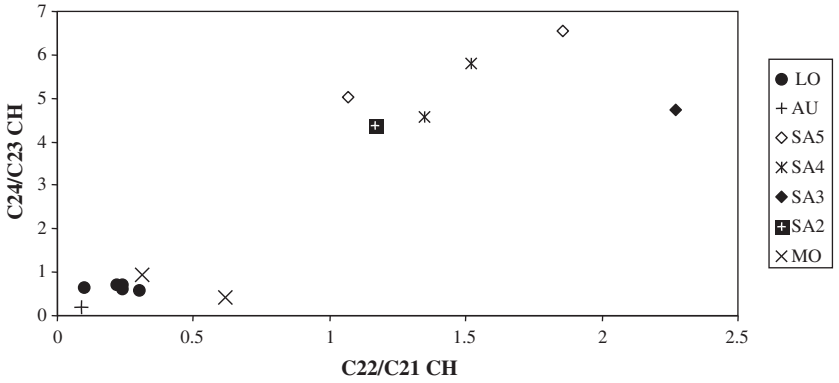

Fig. 16. C_{24}/C_{23} vs. C_{22}/C_{21} cheilanthanes (CH). AU, Late Autunian boghead from Autun; LO, Lodève black shales; MO, Viséan bogheads from Moscow Basin; SA, samples from Odernheim black shale (Autunian from Saar) labelled after hydrological stages described by Müller (2007; see our Fig. 8).

column in lakes (Sinninghe Damsté et al., 1995; Grice et al., 1998; Peters et al., 2005). The gammacerane index, G [10 × gammacerane/(gammacerane + C_{30} hopane)], was calculated after Peters et al. (2005). There was no difference in gammacerane content between the different stages of deposition for the Saar black shale. The origin of gammacerane is uncertain, but it may form via reduction of tetrahymanol, linked to the presence of planktonic ciliates, which are bacteriovorous (Grice et al., 1998). High tetrahymanol abundance occurs in sediments from the eutrophic Lake Lugano (Bechtel and Schubert, 2009b). This was also the case for the Saar

black shales, while a medium abundance occurred in the Lodève black shales. The degree of eutrophication could explain these differences.

While C_{29} steranes are derived mainly from higher plants and C_{27} and C_{28} are commonly associated with the phytoplankton and zooplankton from lacustrine deposits (Huang and Meinschein, 1976, 1979; Philp, 1985), there are many sources of C_{27} and C_{28} steranes and interpretation of their origin must be made with caution (Volkman, 2005). The distribution by sterane carbon number is shown in a ternary plot for humic coals from the Donets Basin (Fig. 17A) and humic coals and lacustrine deposits from the Moscow, Puertollano, Autun, Buxieres, Saar and Lodève basins (Fig. 17B). The C_{27}/C_{29} ratio for the humic coal samples from the Donets Basin ranges from 0.23 to 2.6. C_{29} steranes were more abundant than C_{27} and C_{28} steranes in the coals of the Bashkirian, Kashirian and Podolskian, but less abundant in the Serpukhovian, Vereian, Myachkovian, Kasimovian and Gzhelian coals. The petrographic observations for these samples confirmed only the presence of vitrinite (higher plants) and not the presence of algae in these coals. The C_{27}/C_{29} and C_{28}/C_{29} ratios for the Viséan from the Moscow Basin, humic coals and black shale from the Late Stephanian Puertollano Basin, the Autunian boghead from the Autun Basin and the Autunian black shale and humic coal from the Buxieres, Saar and Lodève basins ranged from 0.3 to 1.3. The petrographic observations for these samples revealed the presence of vitrinite and alginite (*Botryococcus*), confirming the standard interpretation. The ratio values were high in the Puertollano and Saar black shales, peculiarly during the stages 4 and 5 of the lake. McKirdy et al. (1986) indicated a low content of steranes in *B. braunii,* which therefore does not contribute to the sterane content of sediments. Grantham and Wakefield (1988) and Schwark and Empt (2006) studied, respectively, variation in the sterane carbon number distributions of marine source rock-derived crude oils and marine source rocks through geological time. They showed that the C_{27}/C_{29} ratio did not change and the C_{28}/C_{29} ratio increased from the beginning of Mesozoic. This increase is concomitant with an increase in green algae and diverse groups of phytoplankton.

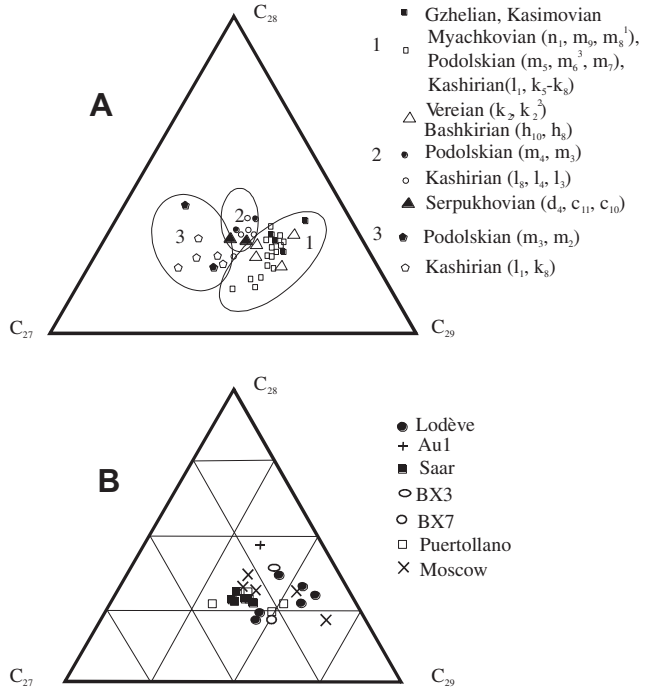

Fig. 17. Sterane plots for humic coals and lacustrine deposits. A, Coals from the Donets Basin; B, Coals and black shale from the Viséan (M, Moscow), Stephanian (Puertollano) and Autunian (AU, Autun; BX, Buxieres; Lodève and Saar).

4.3. Diterpanes – plant speciation and palaeoclimate

Diterpanes are diagnostic of OM sources and palaeoclimate. Schulze and Michaelis (1990) used the diterpanes in a study of German coals, whereby there were differences between the proportion of *ent*-beyerane and *ent*-kaurane in the Late Carboniferous Ruhr and Saar basins (Fig. 18). Philp (1994) described in terms of frequency the relationship between plants and diterpane skeletons as follows: (i) pimaranes occur in gymnosperms and pre-gymnosperms (cordaites) for the Carboniferous, angiosperms, pteridophytes and bryophytes; (ii) *ent*-beyerane in gymnosperms, pre-gymnosperms and angiosperms; (iii) kaurane in angiosperms, gymnosperms, pre-gymnosperms, pteridophytes and bryophytes; and (iv) phyllocladanes in gymnosperms and pre-gymnosperms. Fleck (2001) calculated the diterpane ratio R_{dit}, as (19-norisopimarane + isopimarane + 16α-kaurane)/(*ent*-beyerane + 16β-phyllocladane + 16α-phyllocladane) for the Late Carboniferous coals from the Lorraine Basin. Piedad-Sánchez et al. (2004) also used the ratio for the Late Carboniferous coals of the Asturias Basin.

Two representative distributions are illustrated in Fig. 13 and diterpane ratios are plotted vs. geological age in Fig. 18. The ratio for the Late Carboniferous humic coal samples from the Donets Basin (Izart et al., 2006; Figs. 5 and 18) changes from 0.4 to 2.2. Three groups could be defined for these coals: (i) group 1 with $R_{dit} < 1.1$ and a predominance of phyllocladanes and *ent*-beyerane (Fig. 13), (ii) group 2 with $R_{dit} > 1.5$ and a predominance of kaurane and isopimarane (Fig. 13) and (iii) group 3 with R_{dit} from 1.1 to 1.5 and no dominance of diterpanes. Following the systematics in Fleck (2001), when R_{dit} is >1.5, pteridophytes dominate pre-gymnosperms, which would be linked to a high water table in the swamp. These coals are from the Bashkirian, Podolskian, Myachkovian and lowermost Kasimovian. The climate was probably wetter during these periods. When R_{dit} is <1.1, pre-gymnosperms dominate pteridophytes, which would be linked to a low water table in the swamp and the climate was probably drier during these periods. These coals are from the Serpukhovian, Vereian, lower Kasimovian and Gzhelian. If we compare these data for humic coals from Donets Basin with the Asturias, Ruhr, Lorraine and Saar basins (Fig. 18), the climate was tropical humid during the Moscovian (Westphalian C and D), then dry during the Kasimovian (Early Stephanian).

R_{dit} also can be used for lacustrine deposits, but in this case it conveys information on terrestrial plants living around the lake or aquatic plants as well as palaeoclimate. For the Visean bogheads from the Moscow Basin the ratio was ca. 1.8, corresponding to group 2 with a predominance of kaurane. The Late Stephanian humic coals for Puertollano (Fig. 6), the Autunian boghead from the Autun Basin (Fig. 13) and the Autunian black shales and humic coal from the Buxieres Basin (Fig. 18) range from 1.2 to 3.2, corresponding to groups 2 and 3 with a predominance of kaurane. The values for the lacustrine Autunian from the Saar Basin (Figs. 8 and 13) range from 0.8 to 1.1, corresponding to group 1 with a predominance of kaurane or phyllocladane. The values for the lacustrine Autunian from the Lodève Basin (Fig. 9) range from 0.8 to 1.3 with a predominance of kaurane or phyllocladanes corresponding to groups 1 and 3. Group 1 could often be correlated with group A biomarkers defined by Schlepp et al. (2001) as those with high cheilanthane values.

The source of diterpane contributions in a lake depends on the type of higher plants living in a swamp around the lake and in lake water, which is species dependent on climate. The periods of dryness and wetness (Fig. 18) defined by diterpanes can be compared with the palaeoclimatic periods defined by Schneider et al. (2006) and Roscher and Schneider (2006) from using sedimentology and palaeontology. A wet tropical climate is indicated to have occurred during the Viséan in the Moscow Basin, Late Stephanian (wet B,

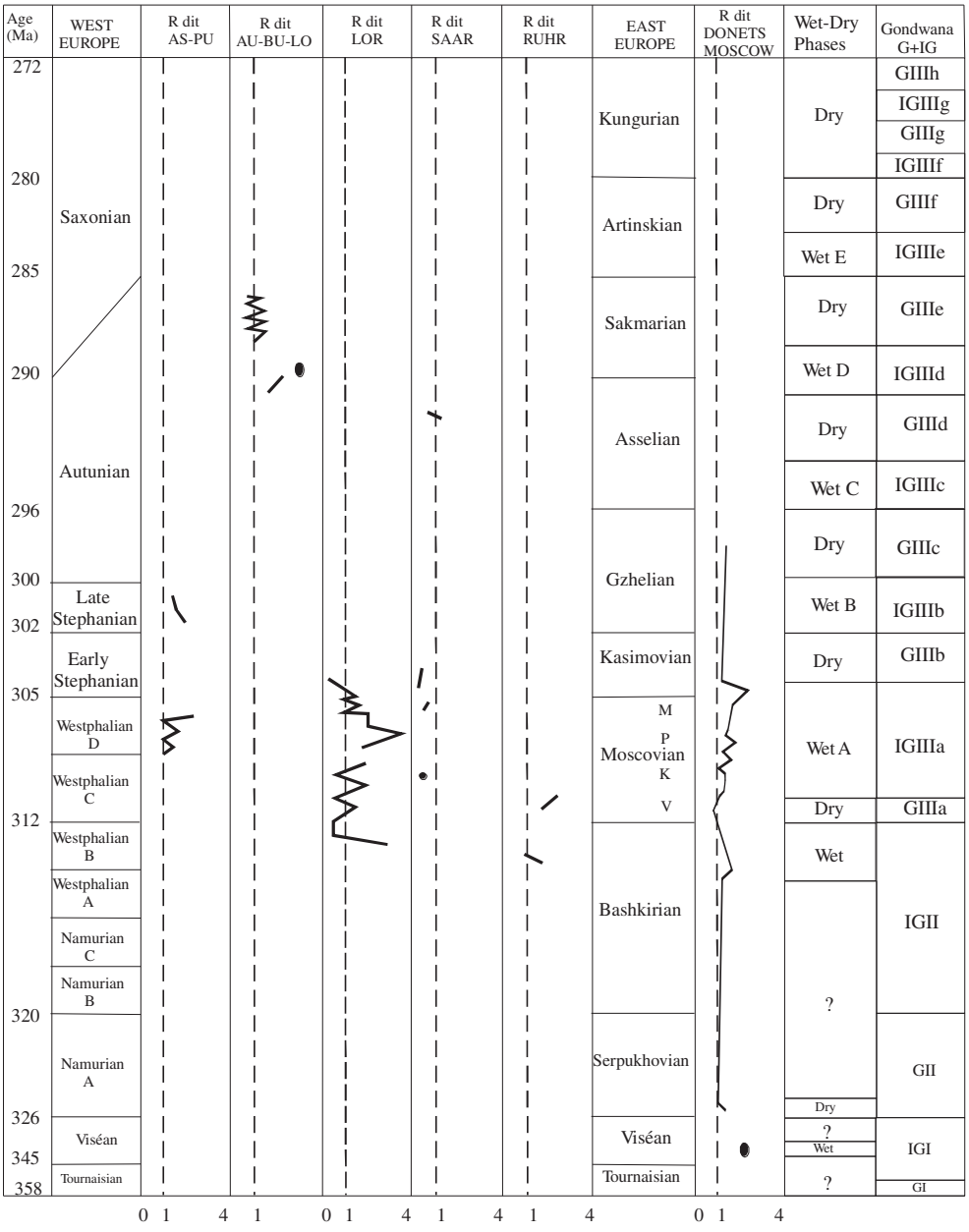

Fig. 18. Changes in diterpanes ratio (R_{dit}) in West Europe (AS, Asturias; AU, Autun; BU, Buxieres; K, Kasimovian; LO, Lodève; LOR, Lorraine; PU, Puertollano; Ruhr, Saar) and East Europe (Moscow, Donets), M, Myachkovian; P, Podolskian; V, Vereian. Wet-dry phases were determined after R_{dit} and A, B, C, D and E corresponds to the wet phases from Roscher and Schneider (2006). G and IG correspond respectively to glacial phase and interglacial phase from Gondwanaland.

Gzhelian) in the Puertollano Basin, and late Autunian (wet D period, Asselian/Sakmarian) in the Buxieres and Autun basins as group 2 and pteridophytes predominate. The contribution from aquatic plants to the diterpanes is certainly higher than from terrestrial plants in the case of the Autunian sample. As group 1 and pregymnosperms predominate, there was probably a dry climate during the Mid-Autunian in the Saar Basin, corresponding to the dry period between the wet C and D periods. As there was an alternation of groups 1 and 3, there was probably a dry climate between the wet D and E periods during the Late Autunian in the Lodève Basin.

All samples showed good agreement between the diterpane ratio and the palaeoclimatic periods defined by Schneider et al. (2006) and Roscher and Schneider (2006). The presence of lacustrine deposits during the dry period of the mid-Autunian in the Saar Basin is not incompatible, since Müller et al. (2006) and Müller (2007) showed from isotope changes that there are different stages in the lacustrine deposits from the Saar Basin (Fig. 8). The diterpanes do not change after the hydrological stages (St 2–5, Fig. 8) defined by Müller et al. (2006), as we observed group 1 corresponding to a dry period for stages 2 and 5 with evaporation equal to water input in lake, stage 3 with evaporation > input and stage 4 with evaporation < input. The contribution of aquatic plants to diterpanes is certainly lower than the terrestrial plant contribution in the case of the Saar samples. Group 1 in the Saar Basin increases in cheilanthanes during all the stages (Fig. 16). Groups 1 and 3 in the Lodève Basin increase in cheilanthanes (Fig. 16) due to a higher productivity from algal blooms and the, development of eutrophic conditions in the lake. The period of higher algal productivity in recent lakes under a temperate and tropical climate is known to result in an increase in P and N content as a result of soil leaching during a wet climate or during an arid climate when the OM is dominated by land-derived OM (Meyers and Lallier-Vergès, 1999; Loizeau et al., 2001; Manalt et al., 2001). Small high frequency cycles of dryness and wetness were

recorded in the cheilanthanes and diterpanes during the late Autunian dry phase in the Lodève Basin. Also, the Autunian black shales from the Saar Basin corresponded to high frequency wet phases during the mid-Autunian arid phase.

4.4. Aromatic biomarkers – plant speciation and palaeoclimate

Numerous aromatic hydrocarbons were identified (Fig. 13, Tables 2 and 3). Retene and cadalene were measured to determine the relative conifer input (Jiang et al., 1998; Van Aarsen et al., 2000; Hautevelle et al., 2006). The retene/cadalene ratio (Fig. 19) was calculated after Hautevelle et al. (2006). Benzo[*a* and *e*]pyrenes were measured as markers of combustion of wood during forest and peat fires (Jiang et al., 1998; Nabbefeld et al., 2010a). Benzo[*e*]pyrene was also attributed to algae by Grice et al. (2007). The ratio benzo[*a* and *e*] pyrenes/cadalene was measured. The arborane/fernane triterpenoid group was also investigated after the study of Vliex et al. (1994) of the Saar Basin (Fig. 19)

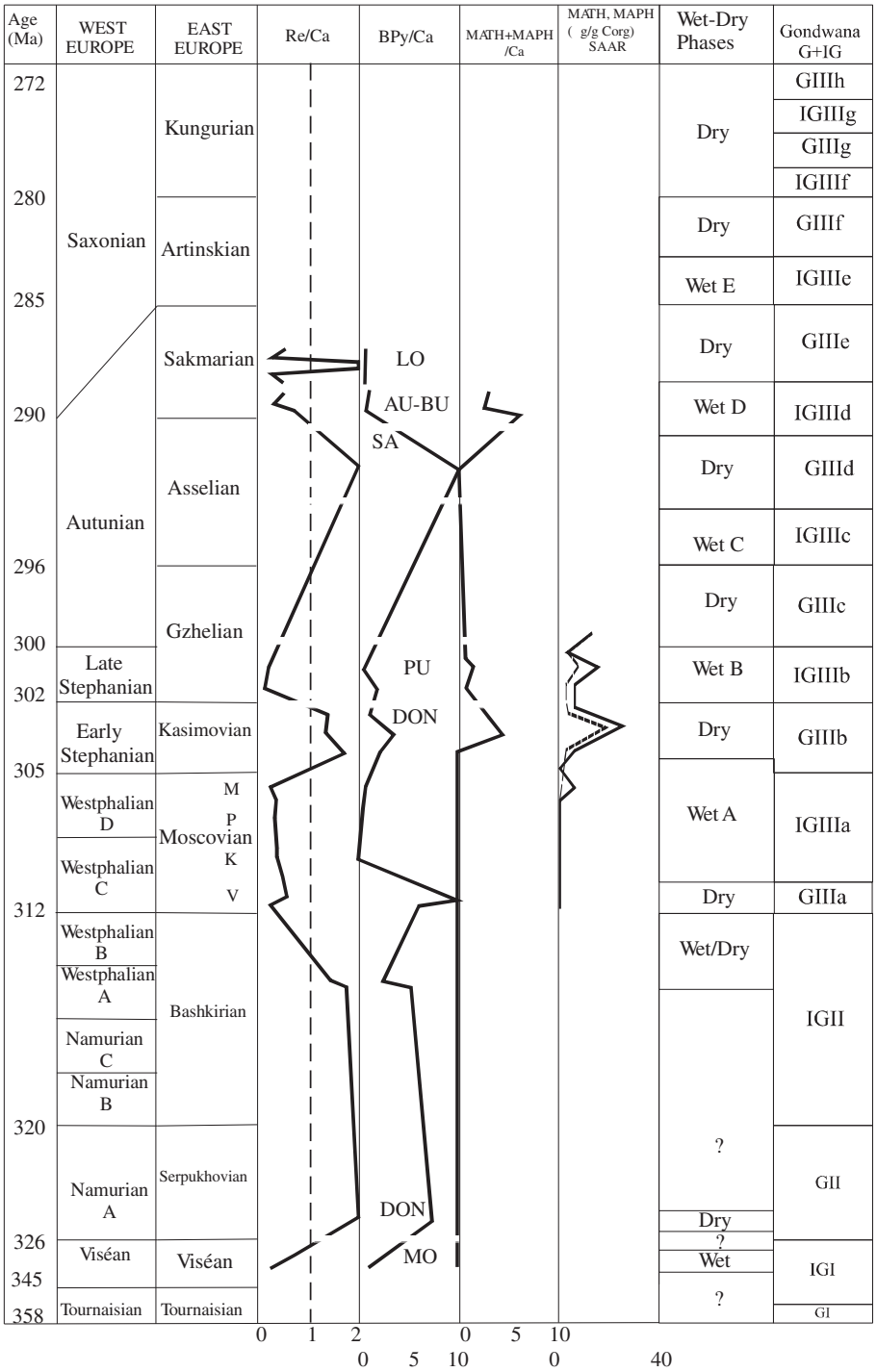

Fig. 19. Change in aromatic ratios during Carboniferous and Permian. AU, Autun; BPy, benzo(a + e)pyrene; BU, Buxieres; Ca, cadalene; DON, Donets; LO, Lodeve; MATH + MAPH, arboranes/fernanes (MATH, MAPH); MO, Moscow; PU: Puertollano; Re, retene; SA, Saar; SAAR, curves from the Saar Basin (Vliex et al., 1994). Wet-dry phases were determined after R_{dit} and A–E corresponds to the wet phases from Roscher and Schneider (2006). G and IG correspond respectively to glacial phase and interglacial phase from Gondwanaland.

and results that showed the appearance of this group from the Stephanian and their probable link with the increase in gymnosperms (Fig. 8) during this period. Monoaromatic tetracyclic hydrocarbons (MATHs) and monoaromatic pentacyclic hydrocarbons (MAPHs) were measured relative to cadalene (MATH + MAPH/cadalene) (Fig. 19). The methyl phenanthrene index (MPI-1) was calculated for maturity.

The first and second maximum in the retene/cadalene ratio (Fig. 19) occurred during the Serpukhovian and Bashkirian, corresponding to the presence of pre-gymnosperms and cordaites in the Donets Basin (Fig. 5), which was also noted in England (Armstroff, 2004). The third maximum could be correlated with the appearance of gymnosperms during the Early Stephanian (Kasimovian) in the Donets Basin (Fig. 5) and the fourth maximum during the mid-Autunian in the Saar Basin concomitant with the increase in gymnosperms (Fig. 8). The Lodève Basin showed during the Late Autunian alternating low and high values of the ratio (Fig. 9). The Viséan of the Moscow Basin, the Moscovian of the Donets Basin (Fig. 5) and the Autunian of the Autun and Buxieres basins (Fig. 7) showed values <1, when cordaites and conifers were absent or in low abundance during the Viséan and Moscovian, and were present during the Autunian but with a lower contribution than in the Saar Basin.

The first, second and third maximum in the benzopyrenes ratio (Fig. 19) occurred in the Serpukhovian, Bashkirian and lower part of the Moscovian, the fourth during the Kasimovian (Early Stephanian) in the Donets Basin and the fifth during the Mid-Autunian in the Saar Basin simultaneously with an increase in inertinite in the coals (Figs. 5 and 8). The ratio corresponds to an increase in peat fires (Jiang et al., 1998) and an increase in combustion temperature in fire (Finkelstein et al., 2005) which is certainly consistent with a dry period. The black shales from the Saar Basin showed high values with low differences between the lacustrine stages. The black shales from the Lodève Basin exhibited low values.

Arboranes and fernanes occurred in samples n3.6 MC and o2 Svet (Fig. 13, Kasimovian, Early Stephanian) from the Donets Basin and the Saar Basin (Vliex et al., 1994), the samples from the Puertollano Basin (Late Stephanian), samples AU1, BX3 and BX7 (Autunian) from the Autun and Buxieres basins but not in the Viséan from the Moscow Basin, the Moscovian (Westphalian) samples from the Donets (Fig. 13) and Saar basins and in the mid-Autunian of the Saar Basin. The maximum in the arboranes/fernanes ratio is linked with the presence of cordaites and gymnosperms (Figs. 5–8), except for the Autunian of the Saar Basin, where Müller (2007) described miospores from cordaites and conifers in black shales. Coals n2.2 and n2.3, located under coal seam n3.3, where the first xerophilous plants (*Autunia* and *Lodevia*) appeared in the Donets Basin, do not contain MATHs and MAPHs, whereas coal n3.6, located above n3.3 coal, showed their first occurrence in the Donets Basin. Auras et al. (2006a,b) showed that these compounds can probably be linked to cordaites and not gymnosperms (*Walchia*). However, some pteridosperms (seed ferns), such as *Autunia* and *Lodevia* observed in the Donets and Autun basins and not studied by these authors, could probably also contribute to the occurrence of these compounds. If we compare the dryness and wetness periods defined by the diterpanes and aromatics, we find the same periods of dryness and wetness (Figs. 18 and 19) as described by Schneider et al. (2006) and Roscher and Schneider (2006). When there is a maximum in diterpanes (Figs. 5, 18 and 19), there is a minimum in benzopyrenes and retene, and vice versa.

5. δD of *n*-alkanes

5.1. Description of δD diagrams from n-alkanes

Three groups of *n*-alkanes were observed (Fig. 20 and Table 2):

(i) Group 1 from C_{13} to C_{21}: the mean δD value is −67‰ for the lacustrine sample AU1 (algae, boghead) and range from −102‰ to −144‰ for the coal samples (higher plants, swamp). The three lacustrine samples from the Saar Basin measured in the Jena laboratory have δD values from −99‰ to −109‰. All samples are depleted in D vs. the two other groups.

(ii) Group 2 from C_{22} to C_{26}: The lacustrine sample AU1 showed a mean δD value of −55‰, while the mean value for the coal samples ranged from −60‰ to −86‰. Three samples from the Saar Basin showed a mean value from −84‰ to −93‰. All samples in group 2 are slightly enriched in D and intermediate between the two other groups.

(iii) Group 3 from C_{27} to C_{35}: For the lacustrine sample AU1, the δD mean valuewas −41‰. For the coal samples, the mean value varied from −70‰ to −110‰. The three Saar Basin samples had a mean from −81‰ to −104‰. All samples in group 3 are enriched in D vs. groups 1 and 2, except for the coals.

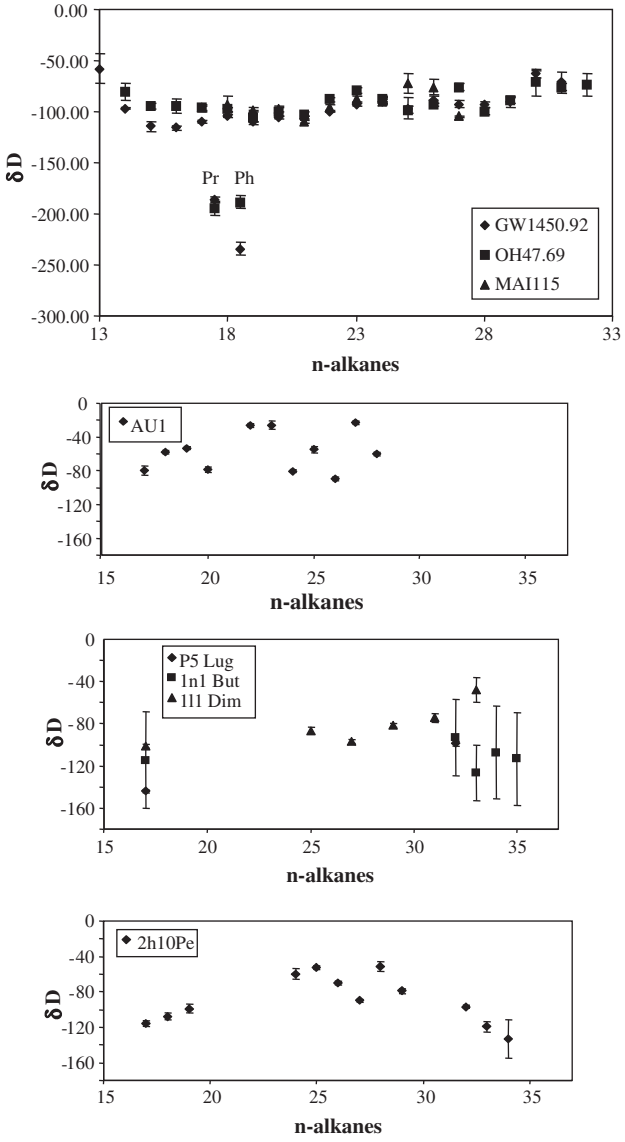

Fig. 20. The δD diagrams for the Saar black shales [GW450.92 (stage 2), MA114.945 (stage 3) and OH47.69 (stage 5)], Autun boghead (AU1) and Donets humic coals (P5 Lug, 1n1 But, 1l1 Dim, h10 M).

The lacustrine samples from the Autun and Saar basins have values more enriched in D for groups 2 and 3 (terrestrial plants) and more depleted in D for group 1 (algae). The coal sample values are depleted in D for groups 1 and 3 from C_{31} to C_{35} and enriched in D for groups 2 and 3 due to C_{27} to C_{30} *n*-alkanes originating from a terrestrial higher plant source.

5.2. Interpretation of δD values from n-alkanes

Temperature changes from lake water or the atmosphere in a swamp are recorded by δD values of *n*-alkanes for recent and ancient sediments (Sauer et al., 2001; Sachse, 2004; Sachse et al., 2004; Dawson et al., 2004). A question remains, however, concerning the impact of maturity on the values. This does not appear to be a problem for samples with VR < 1, a criterion set for our samples (Schwarzkopf and Schoell, 1985; Schimmelmann et al., 2006). Radke et al. (2005) showed a correlation between hydrogen isotope ratio and maturity measured by way of MPI-1 or VRr. The short chain *n*-alkanes are more enriched in D with increasing maturity. The δD values are −126‰ and −108‰, respectively, for a VRr of 0.6% and 0.8% if we use the equation for the Permian Kupferschiefer sample. As the analyzed samples are in this range of VRr, the impact of maturity is certainly low and we conclude that the δD values of the *n*-alkanes (Fig. 20) provide reliable information on the palaeotemperature of the air in the swamps and water in the lakes, as well as palaeoclimate.

If we compare our results with those of Dawson et al. (2004), the values of ca. −100‰ for Carboniferous coals and Permian limnic deposits were close to those for a tropical climate (boghead from Early Carboniferous from Scotland). In constrast, δD values were ca. −200‰, for a glacial or temperate climate (boghead from Permian from Australia). The value for Carboniferous coals could result from extensive evapotranspiration for plants living under a wet tropical climate vs. a temperate climate. This interpretation is confirmed by the potential evapotranspiration measured (Ahn and Tateishy, 1994) for tropical (1500 mm H_2O yr^{-1}), arid (700–1000 mm) and temperate climates (<500 mm). The fact that long and mid-chain *n*-alkanes are more enriched in D than short chain *n*-alkanes could be explained by a difference in the sources of these compounds which are, respectively, trees (arborescent ferns for the Carboniferous swamp) vs. mosses and *Sphagnum* (*Muscites* is known during the Carboniferous). In addition, trees show far greater evapotranspiration than moss. In modern forested wetland peat, *Sphagnum* is like a sponge for water and there is a lower evapotranspiration for moss under the cover of trees than in the trees themselves (Munro, 1984).

During the Early Permian the climate was dry tropical. For such samples, the δD values for the *n*-alkanes derived from lacustrine algae were depleted in D relative to the *n*-alkanes derived from terrestrial higher plants and attributed to the higher evapotranspiration on land than the evaporation from lakes. The values from the Autun and Saar basins exhibit enriched values in D for mid-chain and long chain *n*-alkanes, as for an arid site on the Tibetan plateau (Mügler et al., 2008, 2010; Aichner et al., 2010b), but with a higher enrichment for mid-chain and long chain *n*-alkanes than for short chain *n*-alkanes. A similarity between the relationship of aridity and altitude exists between the Permian lakes located at high altitude in the Hercynian chain and the recent lakes of the Tibetan plateau. Feakins and Sessions (2010) showed that the transpiration factor is more important for D enrichment of leaf water in a semi-arid to arid climate. An alternative hypothesis could be that the xerophytic plants could have drifted via river to the lake and have grown during a dry phase, with an autochthonous algal bloom occurring during a wet phase. Alternating hygrophytic and xerophytic plants have been observed for the Stephanian and Autunian in Europe (Broutin et al., 1986, 1990) and explained by monsoon and dry periods.

6. Conclusions

Organic petrography, Rock–Eval data and biomarkers allowed us to characterize the type of OM in swamp and lake sediments from the Carboniferous and Permian in Europe. The coals deposited in swamps had humic OM formed under oxic conditions. The boghead coals and black shales deposited in lakes showed a mixture of algal and humic OM formed under reducing conditions. Examination of selected diterpanes and aromatic hydrocarbons and the δD of *n*-alkanes provides a further refinement of the depositional setting and palaeoclimate.

A diterpane ratio R_{dit} proposed by Fleck (2001) was compared against the plants known from palaeobotanical studies to be in the swamp or close to the shore of the lake. By knowing the plants in the swamp or close to the shore of the lake, the water table and the palaeoclimate could be determined. When R_{dit} was >1.5, pteridophytes dominated pre-gymnosperms, a condition that would be linked to a high water table in the swamp. When R_{dit} was <1.1, pre-gymnosperms dominated pteridophytes, a condition that would be linked to a low water table in the swamp.

The retene/cadalene ratio used by Hautevelle et al. (2006) as a proxy for conifer input in Jurassic sediments was tested for Carboniferous and Permian deposits. We find that the appearance of xerophytic plants in the Stephanian is recorded in the aromatic hydrocarbons with the retene diagnostic for gymnosperms. We also note that the arborane/fernane ratio is diagnostic for cordaites and probably seed ferns.

During the Carboniferous, the climate was not always tropical wet since some periods of dryness were also evident from the sedimentology, palaeobotany and organic geochemistry. During the Permian, the climate was not always tropical dry, since some periods of wetness associated with monsoons were also recorded. Comparison of aliphatics and aromatics allowed us to propose cycles of wetness and dryness for Europe and a chemostratigraphy during the Carboniferous and Permian, and comparison with the cycles proposed by Roscher and Schneider (2006).

δD measurements of *n*-alkanes can provide information on the palaeotemperature of the air in the swamps and water in the lakes, as well as palaeoclimate. Values of ca. −100‰ for the Carboniferous coals and Permian limnic deposits are close to those reported for a boghead coal from a tropical climate in Scotland (Dawson et al., 2004). These values could result from extensive evapotranspiration for plants living under a wet tropical climate vs. a temperate climate. During the Early Permian the climate was dry tropical. For such samples the values for the *n*-alkanes derived from lacustrine algae were depleted in D relative to the *n*-alkanes derived from terrestrial higher plants, and attributed to the more extensive evapotranspiration on land than evaporation from lakes. An alternative hypothesis could be that xerophytic plants could have drifted via river to the lake and grown during a dry phase, with an autochthonous algal bloom occurring during a wet phase.

Acknowledgements

We thank UMR G2R for financial support for the analyses, I. Volkova for the Moscow samples, the Rhinopolis Association for the Buxières samples, I. Suarez-Ruiz for the Puertollano samples, E. Panova for the Donets samples, A. Müller for the Saar samples, J.-R. Disnar for the Rock-Eval measurements, D. Sachse for the measurements of isotopes in the Jena laboratory on Saar samples, and

D. Molloy (New York State Museum, USA) and K. Grice and an anomymous reviewer for comments and recommendations.

Associate Editor—**C.C. Walters**

References

Ahn, C.H., Tateishy, R., 1994. Estimation of potential evapotranspiration for global data sets. In: Proceeding ISPRS, Communication IV, Symposium, Mapping and Geographic Information System, Athens, Georgia, USA, pp. 586–593.

Aichner, B., Herzschuk, U., Wilkes, H., 2010a. Influence of aquatic macrophytes on the stable carbon isotopic signature of sedimentary organic matter in lakes on the Tibetan Plateau. Organic Geochemistry 41, 706–718.

Aichner, B., Herzschuk, U., Wilkes, H., Vieth, A., Böhner, J., 2010b. δD values of *n*-alkanes in Tibetan lake sediments and aquatic macrophytes – a surface sediment study and application to a 16 Ka record from Lake Koucha. Organic Geochemistry 41, 779–790.

Alsaab, D., Suarez-Ruiz, I., Elie, M., Izart, A., Martinez, L., 2007. Comparison of generative capacities for bitumen and gas between Carboniferous coals from Donets Basin (Ukraine) and a Cretaceous coal from Sabinas–Piedras Negras Basin (Mexico) during artificial maturation in confined pyrolysis system. International Journal of Coal Geology 71, 85–102.

Alsaab, D., Elie, M., Izart, A., Sachsenhofer, R.F., Privalov, V.A., 2008. Predicting methane accumulations generated from humic coals in the Donbas foldbelt (Ukraine). American Association of Petroleum Geologists Bulletin 92, 1029–1053.

Armstroff, A., 2004. Geochemical Significance of Biomarkers in Paleozoic Coals. PhD Thesis, University of Berlin, Germany, 433 pp.

Armstroff, A., Wilkes, H., Schwarzbauer, J., Littke, R., Horsfield, B., 2006. Aromatic hydrocarbons biomarkers in terrestrial organic matter of Devonian to Permian age. Palaeoclimatology, Palaeoecology 240, 253–274.

Audino, M., Grice, K., Alexander, R., Kagi, R.I., 2001a. Macrocyclic-alkanes: a new class of biomarker. Organic Geochemistry 32, 759–763.

Audino, M., Grice, K., Alexander, R., Kagi, R.I., 2001b. Unusual distribution of monomethylalkanes in *Botryococcus braunii*-rich samples: origin and significance. Geochimica et Cosmochimica Acta 65, 1995–2006.

Audino, M., Grice, K., Alexander, R., Kagi, R.I., 2002. Macrocyclic *n*-alkanes: Markers for the freshwater alga *Botryococcus Braunii* in the Gippsland Basin. Australian Petroleum Production and Exploration Association Limited 1, 67–71.

Auras, S., Wilde, V., Hoernes, S., Qcheffler, K., Püttmann, W., 2006a. Biomarker composition of higher plant macrofossils from Late Paleozoic sediments. Palaeogeography, Palaeoclimatology, Palaeoecology 240, 305–317.

Auras, S., Wilde, V., Hoernes, S., Scheffler, K., Püttmann, W., 2006b. Aromatized arborane/fernane hydrocarbons as biomarkers for cordaites. Naturwissenchaften 93, 616–621.

Bangert, B., Stollhofen, H., Lorenz, V., Armstrong, R., 1999. The geochronology and significance of ash-fall tuffs in the glaciogenic Carboniferous–Permian Dwyka group of Namibia and South Africa. Journal of African Earth Sciences 29, 33–49.

Bechtel, A., Schubert, C.J., 2009a. Biogeochemistry of particulate organic matter from lakes of different trophic levels in Switzerland. Organic Geochemistry 40, 441–454.

Bechtel, A., Schubert, C.J., 2009b. A biogeochemical study of sediments from the eutrophicLake Lugano and the oligotrophic Lake Brienz, Switzerland. Organic Geochemistry 40, 1100–1114.

Berner, R.A., 1998. The carbon cycle and CO_2 over Phanerozoc time. Philosophical Transactions of the Royal Society of London B 353, 75–82.

Bingham, E.M., McClymont, E.L., Väliranta, H., Mauquoy, D., Roberts, Z., Chambers, F.M., Pancost, R.D., Evershed, R.P., 2010. Conservative composition of *n*-alkane biomarkers in Sphagnum species: Implications for paleoclimate reconstruction in ombrotrophic peat bog. Organic Geochemistry 41, 214–220.

Broutin, J., Doubinger, J., Langiaux, J., Primey, D., 1986. Conséquences de la coexistence de flores à caractères stéphaniens et autuniens dans les bassins limniques d'Europe occidentale. Mémoires de la Société Géologique de France Nouvelle Série 149, 15–25.

Broutin, J., Doubinger, J., Farjanel, G., Freytet, P., Kerp, H., Langiaux, J., Lebreton, M.-L., Sebban, S., Satta, S., 1990. Le renouvellement des flores au passage Carbonifère Permien: approches stratigraphique, biologique, sédimentologique. Comptes Rendus de l'Académie des Sciences Paris 311 (IIa), 1563–1569.

Buillit, N., Lallier-Verges, E., Disnar, J.-R., Loizeau, J.-L., 1997. Changements climatiques et effets anthropiques au cours du dernier millénaire attesté par l'étude pétrographique de a matière organique (Annecy, le Petit Lac, France). Bulletin de la Société Géologique de France 168, 573–583.

Cecil, C.B., Dulong, F.T., West, R.R., Stamm, R., Wardlaw, B.A., Edgar, N.T., 2003. Climate controls on the stratigraphy of a Middle Pennsylvanian cyclothem in North America. In: Cecil, C.B., Edgar, N.T. (Eds.), Climate Controls on Stratigraphy, vol. 77. SEPM Special Publication, pp. 151–180.

Dawson, D., Grice, K., Wang, S.X., Alexander, R., Radke, J., 2004. Stable hydrogen isotopic composition of hydrocarbons in torbanites (Late Carboniferous to Late Permian) deposited under various climatic conditions. Organic Geochemistry 35, 189–197.

Debriette, P., 1992. Le basin Permien de Bourbon-L'Archambault et le sillon houiller (Allier, France). Bulletin de la Société d'Histoire naturelle et des amis du musée d'Autun 144, 11–34.

Del Rio, J.C., Garcia-Molla, J., Gonzales-Vila, F.J., Martin, F., 1994. Composition and origin of the aliphatic extractable hydrocarbons in the Puertollano (Spain) oil shale. Organic Geochemistry 21, 897–909.

Dercourt, J., Gaetani, M., Vryelinck, B., Barrier, E., Biju-Duval, B., Brunet, M.F., Cadet, J.P.,Crasquin, S., Sandulescu, M. (Eds.), 2000. Atlas Peri-Tethys Palaeogeographical Maps.CCGM/CGMW, Paris, 24 Maps and Explanatory Notes.

Derenne, S., Largeau, C., Behar, F., 1994. Low polarity products of Permian to Recent *Botryococcus*-rich sediments: first evidence for the contribution of an isoprenoid algaenan to kerogen formation. Geochimica et Cosmochimica Acta 58, 2703–3711.

Derenne, S., Largeau, C., Casadevall, E., Connan, J., 1998. Comparison of torbanite of various origins and evolutionary stages. Bacterial composition to their formation. Cause of lack of botryococcane in bitumens. Organic Geochemistry 12, 43–59.

Doubinger, J., Elsass, F., 1975. Nouvelles données minéralogiques et palynologiques sur les sédiments permiens du bassin d'Autun. Bulletin de la Société d'Histoire naturelle et des amis du musée d'Autun 76, 13–28.

Eglinton, G., Hamilton, R.J., 1967. Leaf epiciticular waxes. Science 156, 1322–1335.

Eglinton, G., Gonzales, A.G., Hamilton, R.J., Raphael, R.A., 1962. Hydrocarbon constituents of the wax coatings of plant leaves: a taxonomic survey. Phytochemistry 1, 89–102.

Espitalié, J., Deroo, G., Marquis, F., 1985a. La pyrolyse Rock-Eval et ses applications. Première partie. Revue de l'Institut français du Pétrole 40, 563–579.

Espitalié, J., Deroo, G., Marquis, F., 1985b. La pyrolyse Rock-Eval et ses applications. Deuxième partie. Revue de l'Institut français du Pétrole 40, 755–784.

Espitalié, J., Deroo, G., Marquis, F., 1986. La pyrolyse Rock-Eval et ses applications. Troisième partie. Revue de l'Institut français du Pétrole 41, 73–89.

Feakins, S.J., Sessions, A.L., 2010. Controls on the D/H ratios of plant leaf waxes in an arid ecosystem. Geochimica et Cosmochimica Acta 74, 2128–2141.

Ficken, K.J., Li, B., Swain, D.L., Eglinton, G., 2000. A *n*-alkane proxy for the sedimentary input of submerged/floating freshwater aquatic macrophytes. Organic Geochemistry 31, 745–749.

Finkelstein, D.B., Pratt, M.P., Curtin, T.M., Brassel, S.C., 2005. Wildfires and seasonal aridity recorded in Late Cretaceous strata from south-eastern Arizona, USA. Sedimentology 52, 587–599.

Fleck, S., 2001. Corrélation entre Géochimie Organique, Sédimentologie et Stratigraphie Séquentielle pour la Caractérisation des Paléoenvironnements de Dépôt. PhD Thesis, Université Henri Poincaré, Nancy, France, 387 pp.

Fleck, S., Michels, R., Izart, A., Elie, M., Landais, P., 2001. Paleoenvironmental assessment of Westphalian fluvio-lacustrine deposits of Lorraine (France) using a combination of organic geochemistry and sedimentology. International Journal of Coal Geology 48, 65–88.

Gibbs, M.T., Rees, P.McA., Kutzbach, J.E., Ziegler, A.M., Behrling, P.J., Rowley, D.B., 2002. Simulations of Permian climate and comparisons with climate-sensitive sediments. The Journal of Geology 110, 33–55.

Golonka, J., Ross, M.I., Scotese, C.R., 1995. Phanerozoic paleogeographic and paleoclimatic modelling maps. Canadian Society of Petroleum Geologists Memoir 17, 1–47.

Grantham, P.J., Wakefield, L.L., 1988. Variations in the sterane carbon number distributions of marine source rock derived crude oils through geological time. Organic Geochemistry 12, 61–73.

Grice, K., Schouten, S., Peters, K.E., Sinninghe-Damsté, J.S., 1998. Molecular isotopic characterization of hydrocarbon biomarkers in Paleocene–Eocene evaporitic lacustrine source rocks from the Jianghan Basin, China. Organic Geochemistry 29, 1745–1764.

Grice, K., Audino, M., Boreham, C.J., Alexander, R., Kagi, R.I., 2001. Distributions and stable carbon isotopic compositions of biomarkers in torbanites from different paleogeographical locations. Organic Geochemistry 32, 1195–1210.

Grice, K., Nabbefeld, B., Maslen, E., 2007. Source and significance of selected poycyclic aromatic hydrocarbons in sediments (Hovea-3 well, Perth Basin, Western Australia) spanning the Permian–Triassic boundary. Organic Geochemistry 38, 1795–1803.

Han, Z., Kruge, M.A., 1999. Classification of torbanite and cannel coal. II. Insights from pyrolysis-GC/MS and multivariate statistical analysis. International Journal of Coal Geology 38, 203–218.

Han, Z., Kruge, M.A., Crelling, J.C., Stankiewicz, B.A., 1995. Organic geochemical characterization of the density fractions of a Permian torbanite. Organic Geochemistry 21, 39–50.

Han, Z., Kruge, M.A., Crelling, J.C., Bensley, D.F., 1999. Classification of torbanite and cannel coal. I. Insights from petrographic analysis of density fractions. International Journal of Coal Geology 38, 181–202.

Hautevelle, Y., Michels, R., Malartre, F., Trouiller, A., 2006. Vascular plant biomarkers as proxies of paleoflora and paleoclimatic changes at the Dogger/Malm transition of Paris Basin (France). Organic Geochemistry 37, 610–625.

Huang, W.Y., Meinschein, W.G., 1976. Sterols as source indicators of organic materials insediments. Geochimica et Cosmochimica Acta 40, 323–330.

Huang, W.Y., Meinschein, W.G., 1979. Sterols as ecological indicators. Geochimica et Cosmochimica Acta 43, 739–745.

Iannuzi, R., Rösler, O., 2000. Floristic migration in South America during the Carboniferous: phytogeographic and biostratigraphic implications. Palaeogeography, Palaeoclimatology, Palaeoecology 161, 71–94.

Inosova, K.I., Kruzina, A.H., Schvatsman, E.G., 1975. Atlas of miospores and pollens fromthe Upper Carboniferous and Lower Permian of the Donets Basin. Nedra, Moscow, 176 pp. (in Russian).

Izart, A., Vaslet, D., Briand, C., Broutin, J., Coquel, R., Davydov, V., Donsimoni, M., El Wartiti, M., Ensepbaev, T., Geluk, M., Goreva, N., Görür, N., Iqbal, N., Joltaev, G.,

Kossovaya, O., Krainer, K., Laveine, J.-P., Makhlina, M., Maslo, A., Nemirovskaya, T., Kora, M., Kozitskaya, R., Massa, D., Mercier, D., Monod, O., Oplustil, S., Schneider, J., Schönlaub, H.,Stschegolev, A., Süss, P., Vachard, D., Vai, G.B., Vozarova, A., Weissbrod, T., Zdanowski, A., 1998. Stratigraphic correlations between the continental and marine Tethyanand Peri-Tethyan basins during the Late Carboniferous and the Early Permian. In: Crasquin-Soleau, S., Izart, A., Vaslet, D., De Wever, P. (Eds.), Peri-Tethys: Stratigraphic Correlations 2. Geodiversitas 20, 4, pp. 521–595.

Izart, A., Stephenson, R., Vai, G.B., Vachard, D., Le Nindre, Y., Vaslet, D., Fauvel, P.-J., Süss, P., Kossovaya, O., Chen, Z., Maslo, A., Stovba, S., 2003. Sequence stratigraphy and Correlation of the Late Carboniferous and Permian in CIS, Europe, Tethyan area, North Africa, China, Gondwanaland and USA. Palaeogeography, Palaeoclimatology, Palaeoecology 196, 59–84.

Izart, A., Palain, C., Malartre, F., Fleck, S., Michels, R., 2005. Palaeoenvironments, paleoclimates and sequences of Westphalian deposits of Lorraine coal Basin (Upper Carboniferous, NE France). Bulletin de la Société géologique de France 176 (3), 301–315.

Izart, A., Sachsenhofer, R.F., Privalov, V.A., Elie, M., Panova, E.A., Antsiferov, V.A., Alsaab, D., Sotirov, A., Zdravkov, A., Zhykaliak, M.V., 2006. Stratigraphic distribution of macerals and biomarkers in the Donets Basin: implications for paleoecology, paleoclimatology and eustacy. International Journal of Coal Geology 66, 69–107.

Jaraula, C., Grice, K., Vitzthum von Eckstaedt, C., Twitchett, R., Wignall, P., Kelly, D., 2010. Stable carbon and hydrogen isotopes of components derived from controlled burning experiments of C_3 and C_4 plants and their use as environmental proxies for tracking fire history. Australian Organic Geochemistry Conference, Canberra, December 2010.

Jaraula, C., Grice, K., Vitzthum von Eckstaedt, C., Twitchett, R., Wignall, P., Kelly, D., 2011. Stable carbon and hydrogen isotopes of components derived from controlled burning experiments of C_3 and C_4 plants and their use as environmental proxies for tracking fire history. The Australian and New Zealand Society for Mass Spectrometry, Perth, February 2011.

Jiang, C., Alxander, R., Kagi, R.F., Murray, A.P., 1998. Polycyclic aromatic hydrocarbons in ancient sediments and their relationships to paleoclimate. Organic Geochemistry 29, 1721–1735.

Jimenez, A., Martinez-Tarazona, R., Suarez-Ruiz, I., 1999. Paleoenvironmental conditions of Puertollano coals (Spain): petrological and geochemical study. International Journal of Coal Geology 41, 189–211.

Kruge, M.A., Suarez-Ruiz, I., 1991. Organic geochemistry and petrography of Spanish oil shales. Fuel 70, 1298–1302.

Kruge, M.A., Hubert, J.F., Jay Akes, R., Meriney, P.E., 1990. Biological markers in Lower Jurassic synrift lacustrine black shales, Hartford basin, Connecticut, USA 1990. Organic Geochemistry 15, 281–289.

Kuhn, J.K., Krull, E.S., Bowater, A., Grice, K., Gleixner, G., 2010. The occurrence of short chain *n*-alkanes with an even over odd predominance in higher plants and soils. Organic Geochemistry 41, 88–95.

Kutzbach, J.E., Ziegler, A.M., 1993. Simulation of the late Permian climate and biomes with an atmosphere-ocean model: comparisons with observations. Philosophical Transactions of the Royal Society of London 341 (B), 327–340.

Kutzbach, J.E., Ziegler, A.M., 1994. Simulation of Late Permian climate and biomes with an atmospheric-ocean model; comparison with observations. In: Allen, J.R.L., Hoskins, B.J., Sellwood, B.W., Spicer, R.A., Valdes, P.J. (Eds.), Paleoclimates and their Modelling, with Special Reference to the Mesozoic Era. Chapman and Hall, London, pp. 119–132.

Loizeau, J.-L., Span, D., Coppee, V., Dominik, J., 2001. Evolution of trophic state of Lake Annecy (eastern France) since the last glaciation as indicated by iron, manganese and phosphorus speciation. Journal of Paleolimnology 25, 205–214.

Lopez-Gamundi, O.R., 1997. Glacial-postglacial transition in the late Paleozoic basins of southern south America. In: Martini, I.P. (Ed.), Late Glacial and Postglacial Environments Changes, Quaternary, Carboniferous–Permian and Proterozoic. Oxford University Press, pp. 147–168.

Makhlina, M.K., Vdovenko, M.V., Alekseev, A.S., Byvshcheva, T.V., Donakova, L.M., Zhulitova, V.E., Kononova, L.I., Umnova, N.I., Shik, E.M., 1993. Early Carboniferous of the Moscow syncline and Voronezh anteclise. Rossiiskaya Akademiya Nauk, Moskva Nauka, 1–223.

Manalt, F., Beck, C., Disnar, J.-R., Deconinck, J.-F., Recourt, P., 2001. Evolution of clay mineral assemblages and organic matter in the Late glacial–Holocene sedimentary infill of Lake Annecy (northwestern Alps): palaeoenvironmental implications. Journal of Paleolimnology 25, 179–192.

Marteau, P., 1983. Le bassin permo-carbonifère d'Autun, stratigraphie, sédimentologie et aspects structuraux. Documents du Bureau de Recherches Géologiques et Minières 64, 198.

McKirdy, D.M., Cox, R.E., Volkman, J.K., Howell, V.J., 1986. Botryococcane in a new class of Australian non-marine crude oils. Nature 320, 57–59.

McKirdy, D.M., Krull, E., Mee, A., Haynes, D., Thorpe, C., Webster, L., Grice, K., Gell, P., 2010. Natural and cultural eutrophication in the Coorong, South Australia. Organic Geochemistry 41, 96–110.

Menning, M., Hendrich, A. (Eds.), 2002. Stratigraphic Table of Germany. Deutsche Stratigraphische Kommission, Forschunginstitut Senckenberg, Frankfurt, Germany.

Meyers, P.A., Lallier-Vergès, E., 1999. Lacustrine sedimentary organic matter records of Late Quaternary paleoclimates. Journal of Paleolimnology 21, 345–372.

Mügler, I., Sachse, D., Werner, M., Xu, B., Wu, G., Yao, T., Gleixner, G., 2008. Effect of lake evaporation on δD values of lacustrine *n*-alkanes: a comparison of Nam Co (Tibetan Plateau) and Holzmaar (Germany). Organic Geochemistry 39, 711–729.

Mügler, I., Gleixner, G., Günther, F., Maüsbacher, R., Daut, G., Schütt, B., Berking, J., Schwalb, H., Schwark, L., Xu, B., Yao, T., Zhu, L., Yi, C., 2010. A multi-proxy approach to reconstruct hydrological changes and Holocene climate development in Nam Co, central Tibet. Journal of Paleolimnology 43, 625–648.

Müller, A.B., 2007. Klimatische und Biogeochemische Entwicklung Lakustriner Systeme aus den Rotliegend des Saar–Nahe-Beckens (SW Deutschland): Ein Multidisziplinärer Ansatz. PhD Thesis, Münster Universität, Germany, 163 pp.

Müller, A.B., Strauss, H., Hartkopf-Fröder, C., Littke, R., 2006. Reconstructing the evolution of the latest Pennsylvanian–earliest Permian lake Odernheim based on stable isotope geochemistry and palynofacies: a case study from the Saar–Nahe Basin, Germany. Palaeogeography, Palaeoclimatology, Palaeoecology 240, 204–224.

Munro, D.S., 1984. Summer soil moisture content and the water table in a forested wetland peat. Canadian Journal of Forest Resources 14, 331–335.

Nabbefeld, B., Grice, K., Summons, R.E., Hays, L., Cao, C., 2010a. Significance of polycyclic aromatic hydrocarbons (PAHs) in Permian/Triassic boundary sections. Applied Geochemistry 25, 1374–1382.

Nabbefeld, B., Grice, K., Twitchett, R.J., Summons, R.E., Hays, L.E., Böttcher, M.E., Asif, M., 2010b. An integrated biomarker, isotopic and palaeoenvironmental study through the Late Permian event at Lusitaniadalen, Spitsbergen. Earth and Planetary Sciences Letters 291, 84–96.

Ourisson, G., Albrecht, P., Maxwell, J.R., Wheatly, R.E., 1979. The hopanoids. Paleochemistry and biochemistry of a group of natural products. Pure and Applied Chemistry 51, 709–729.

Ourisson, G., Albrecht, P., Rohmer, M., 1984. The microbial origin of fossil fuels. Scientific American 251, 44–51.

Paquette, Y., Doubinger, J., Courel, L., 1980. Etude palynologique de la couche du toit du bassin autunien de l'Aumance (Assise de Buxieres); liaison avec les milieux sédimentaires. Bulletin de la Société d'Histoire naturelle et des ammis du musée d'Autun 95, 85–101.

Parrish, J.T., 1993. Climate of the supercontinent Pangea. Journal of Geology 101, 215–233.

Parrish, J.T., 1995. Geologic evidence of Permian climate. In: Scholle, P.A., Peryt, T.M., Scholle, D.S. (Eds.), The Permian of Northern Pangea, Paleogeography, Paleoclimates, Stratigraphy, vol. 1. Springer, Berlin, pp. 54–61.

Peters, K.E., Walters, C.C., Moldowan, J.M., 2005. The Biomarker Guide, Biomarkers and Isotopes in Petroleum Exploration and Earth History, second ed., vol. 2. Cambridge University Press. 1155 pp.

Peyser, C.E., Poulsen, C.J., 2008. Controls on Permo-Carboniferous precipitation over tropical Pangea: a GCM sensitivity study. Palaeogeogrphy, Palaeoclimatology, Palaeoecology 268, 181–192.

Philp, R.P., 1985. Fossil Fuel Biomarkers. Methods in Geochemistry and Geophysics, vol. 23. Elsevier, New York, 294 pp..

Philp, R.P., 1994. Geochemical characteristics of oils derived predominantly from terrigenous source materials. In: Scott, A.C., Fleet, A.J. (Eds.), Coal and Coal Bearing Strata as Oil-Prone Source Rocks? The Geological Society, vol. 77. Special Publication, London, pp. 71–91.

Piedad-Sánchez, N., Suárez-Ruiz, I., Martinez, L., Izart, A., Elie, M., Keravis, D., 2004. Organic petrology and geochemistry of the Carboniferous coal seams from the CentralAsturian Coal Basin (NW Spain). International Journal of Coal Geology 57, 211–242.

Radke, J., Willsch, H., Leythaeuser, Teichmüller, M., 1982. Aromatic components of coal: relation of distribution pattern to rank. Geochimica et Cosmochimica Acta 46, 1831–1848.

Radke, J., Bechtel, A., Gaupp, R., Püttmann, W., Schwark, L., Sachse, D., Gleixner, G., 2005. Correlation between hydrogen isotope ratios of lipid biomarkers and sediment maturity. Geochimica et Cosmochimica Acta 69, 5517–5530.

Revill, A.T., Volkman, J.K., O'Leary, T., Summons, R.E., Boreham, C.J., Banks, M.R., Denver, K., 1994. Hydrocarbon markers, thermal maturity and depositional setting of tasmanite oil shales from Tasmania, Australia. Geochimica et Cosmochimica Acta 68, 3803–3822.

Rieley, G., Collier, R.J., Jones, D.H., Eglinton, G., Ealin, P.A., Fallick, A.E., 1991. Sources of sedimentary lipids deduced from stable carbon-isotope analyses of individual compound. Nature 352, 425–427.

Roscher, M., Schneider, J.W., 2006. Permocarboniferous climate: Early Pennsylvanian to Late Permian climate development of central Europe in a regional and global context. In: Lucas, S.G., Cassini, G., Schneider, J.W. (Eds.), Non Marine Permian Chronology and Correlation, vol. 265. The Geological Society of London, pp. 5–136.

Roscher, M., Berner, U., Schneider, J.W., 2008. A tool for the assessment of the paleo distribution of source and reservoir rocks. Oil ang Gas European Magazine 3, 131–137.

Sachse, D., 2004. Compound-Specific Hydrogen Isotope Ratios of Sedimentary *n*-Alkanes: A New Paleoclimate Proxy. PhD Thesis, Jena Universität, Germany, 77 pp.

Sachse, D., Radke, J., Gleixner, G., 2004. Hydrogen isotope ratios of recent lacustrine sedimentary *n*-alkanes record modern climate variability. Geochimica et Cosmochimica Acta 68, 23, 4877–4889.

Sachsenhofer, R.F., Privalov, V.A., Izart, A., Elie, M., Kortensky, J., Panova, E.A., Sotirov, A., Zhykalyak, M.V., 2003. Petrography and geochemistry of coal seams in the Donets Basin (Ukraine): implications for paleoecology. International Journal of Coal Geology 55, 225–259.

Sauer, P.E., Eglinton, T.L., Hayes, J.M., Schimmelmann, A., Sessions, A.L., 2001. Compound-specific D/H ratios of lipid biomarkers from sediments as a proxy forenvironmental and climatic conditions. Geochimica et Cosmochimica Acta 65, 213–222.

Schimmelmann, A., Sessions, A.L., Mastalerz, M., 2006. Hydrogen isotope (D/H) composition of organic matter during diagenesis and thermal maturation. Annual Review of Earth and Planetary Sciences 34, 501–533.

Schlepp, L., Landais, P., Elie, M., Faure, P., 2001. Influence of paleoenvironment and radiolytic alteration on the geochemistry of organic matter from Autunian shales of the Lodève uranium deposit, France. Bulletin de la Société géologique de France 171, 92–109.

Schneider, J.W., Körner, F., Roscher, M., Kroner, V., 2006. Permian climate development in the northern peri-tethys – the Lodève basin, French Massif Central, compared in a European and global context. Palaeogeography, Palaeoclimatology, Palaeoecology 240, 161–183.

Schulze, T., Michaelis, Z., 1990. Structure and origin of terpenoid hydrocarbons in some German coals. Organic Geochemistry 16, 1051–1058.

Schwark, L., Empt, P., 2006. Sterane biomarkers as indicators of Palaeozoic algal evolutionand extinction events. Palaeogeography, Palaeoclimatology, Palaeoecology 240, 225–236.

Schwarzkopf, T., Schoell, M., 1985. Die Variation der C- und H-Isotopenverhältnisse in Kohlen und deren Abhängigkeit von der Maceralzusammensetzung und Inkohlungsgrad. Fortschrift Geologie Rheinland und Westfalen 33, 161–168.

Scotese, C.R., McKerrow, W.S., 1990. Revised World maps and introduction. In: McKerrow, W.S., Scotese, C.R. (Eds.), Palaeozoic Palaeogeography and Biogeography, vol. 12. The Geological Society of London Memoir, pp. 1–21.

Sinninghe Damsté, J.S., Van Duin, A.C.T., Hollander, D., Kohnen, M.E.L., De Leeuw, J.W., 1995. Early diagenesis of bacteriohopanpolyol derivatives: formation of fossils homohopanoids. Organic Geochemistry 59, 5141–5147.

Stollhofen, H., Stanistreet, I.G., Bangert, B., Grill, H., 2000. Tuffs, tectonism and glacially related sea-level changes, Carboniferous–Permian, southern Namibia. Palaeogeography, Palaeoclimatology, Palaeoecology 161, 127–150.

Vai, G.B., 2003. Development of the paleogeography of Pangea from Late Carboniferous to Early Permian. Palaeogeography, Palaeoclimatology, Palaeoecology 196, 125–155.

Van Aarsen, B.F.K., Alexander, R., Kagi, R., 2000. Higher plant biomarkers reflect paleovegetation changes during Jurassic time. Geochimica et Cosmochimica Acta 64, 1417–1424.

Visser, J.N.J., 1997. A review of the Permo-Carboniferous glaciation in Africa. In: Martini, I.P. (Ed.), Late Glacial and Postglacial Environments Changes, Quaternary, Carboniferous–Permian and Proterozoic. Oxford University Press, pp. 169–191.

Vliex, M., Hagemann, H.W., Püttmann, W., 1994. Aromatized arborane/fernanehydrocarbons as molecular indicator of floral changes in Upper Carboniferous/Lower Permian strata of the Saar–Nahe Basin, South West Germany. Geochimica et Cosmochimica Acta 58, 4689–4702.

Volkman, J.K., 2005. Sterols and other triterpenoids: source specificity and evolution of biosynthetic pathways. Organic Geochemistry 36, 139–159.

Volkova, I.B., 1975. The types of coal seams of the Carboniferous and their distribution over the territory of the USSR. Report of the 17th International Congress on the stratigraphy ofCarboniferous, Krefeld, 1971, pp. 327–341.

Wollenweber, J., Schwarzbauer, J., Littke, R., Wilkes, H., Armstroff, A., Horsfield, B., 2006. Characterization of non-extractable macromolecular organic matter in Paleozoic coals. Palaeoclimatology, Palaeoecology 240, 275–304.

Yamamoto, C., Kawamura, K., Seki, O., Meyers, P.A., Zheng, Y., Zhou, W., 2010. Paleoenvironmental significance of compound-specific $\delta^{13}C$ variations in *n*-alkanes in theHongyuan peat sequence from southwest China over the last 13 Ka. Organic Geochemistry 41, 491–497.

Yawanarajah, S.R., Kruge, M.A., Mastalerz, M., Sliwinski, W., 1993. Organic geochemistry of Permian organic-rich sediments from the Sudetes area, SW Poland. Organic Geochemistry 20, 267–281.

Zhang, Z., Metzger, P., Sachs, J.P., 2007. Biomarker evidence for the co-occurrence of three races (A, B and C) of *Botryococcus braunii* in El Junco Lake, Galapagos. Organic Geochemistry 38, 1459–1478.

Zhou, Y., Grice, K., Stuart-Williams, H., Farquhar, G.D., Hocart, C.H., Lu, H., Liu, W., 2010. Biosynthetic origin of the saw-toothed profile in ^{13}C of *n*-alkanes and systematic isotopic differences between iso- and anteiso-alkanes in leaf waxes of land plants. Phytochemistry 71, 388–403.

Ziegler, A.M., 1990. Phytogeographic patterns and continental configurations during thePermian Period. In: McKerrow, W.S., Scotese, C.R. (Eds.), Palaeozoic Palaeogeography and Biostratigraphy, vol. 12. Geological Society of London Memoir, pp. 363–379.